FICE ATLAS

Academic Research Report for Health Care Professionals

Atlas of Spectral Endoscopic Images

Supervised by Yoichi Miyake, Research Center for Frontier Medical Engineering, Chiba University
Edited by Teruo Kouzu, Department of Endoscopic Diagnostics and Therapeutics, Chiba University Hospital

Atlas of Spectral Endoscopic Images

First edition

FUJINON
FUJIFILM

SEG-086-00 FICE ATLAS case files
Printed in Japan 2008.6.DA 5000

Preface

FICE (Flexible spectral Imaging Color Enhancement) is an image processing function optionally available with the VP-4400, an endoscope processor distributed by Fujinon Corporation. The development of this technology was started as a research theme at the Research Center for Frontier Medical Engineering (CFME), Chiba University, in Spring 2004, and I was involved in the development of this technology from the preliminary stage. When I used computer simulation to process and display an image of the oral mucosa for the first time, I felt confident that the technology would work effectively. I still remember my impression clearly. When I entered into the world of spectral endoscopy, I somewhat regretted having observed the gastrointestinal tract with conventional white light.

Since the late 1990s, researchers at the Department of Endoscopic Diagnostics and Therapeutics have been collecting and analyzing basic data on the relationship between gastrointestinal lesions and their scattering spectra and have seen the substantial potential. I, as an editor, am deeply impressed by the practical application of the technology as a clinically useful modality.

FICE, a technology based on spectral estimation theory, is not easy to understand for everyone. Because of its flexibility in setting parameters, first-time users may have difficulty in selecting the optimal settings for the intended use; however, further development and application are expected.

I asked Professor Yoichi Miyake, a developer of FICE technology and the director of CFME, Chiba University, for an explanation of the basic principle of FICE for publication in this atlas. I also asked frontline physicians for descriptions of cases with photographs, outcomes, and their own wavelength settings, or their expertise. I hope these documents and data will help other physicians use FICE more effectively and contribute to the improvement in the quality of endoscopic treatment.

I gratefully acknowledge the busy physicians for providing and describing FICE images in a timely manner. I also thank the personnel at Fujinon Toshiba ES Systems Co., Ltd., and Fujinon Corporation for their cooperation in planning and editing the case series.

October 2007

Prof. Teruo Kouzu, Department of Endoscopic Diagnostics and Therapeutics,
Chiba University Hospital

Table of Contents

Contributors to the FICE Atlas (this case series)

(Listed in publication order)

- Shigeto Yoshida, Department of Endoscopy, Hiroshima University Hospital
- Teruo Kouzu, Director and Professor, Department of Endoscopic Diagnostics and Therapeutics, Chiba University Hospital
- Hiroyuki Osawa, Assistant Professor, Division of Gastroenterology, Department of Internal Medicine, Jichi Medical University
- Mitsuyo Yoshizawa, Division of Gastroenterology, Department of Internal Medicine, Jichi Medical University
- Masahito Inoue, Department of Endoscopic Diagnostics and Therapeutics, Chiba University Hospital
- Shoji Mitsufuji, Assistant Professor, Department of Molecular Gastroenterology and Hepatology, Kyoto Prefectural University of Medicine Graduate School of Medical Science
- Kazutomo Togashi, Assistant Professor, Division of Endoscopy, Jichi Medical University
- Hideki Mitooka, Director, Ashiya Mitooka Clinic
- Miwako Arima, Deputy Director, Department of Gastroenterology, Saitama Cancer Center
- Tomonori Yano, Division of Gastroenterology, Department of Internal Medicine, Jichi Medical University
- Hideo Yanai, Director, Department of Gastroenterology & Hepatology, National Hospital Organization Kanmon Medical Center
- Yukari Tanioka, Department of Gastroenterology & Hepatology, National Hospital Organization Kanmon Medical Center
- Tetsumaru Miyawaki, Director, Izumo Central Clinic

Supervised by Yoichi Miyake, Director, Research Center for Frontier Medical Engineering, Chiba University

Edited by Teruo Kouzu, Director and Professor, Department of Endoscopic Diagnostics and Therapeutics, Chiba University Hospital (also serving as Deputy Director, Research Center for Frontier Medical Engineering, Chiba University)

Principle of FICE

This chapter describes the principle of FICE, focusing on the relationship between color information (spectral information) and clinical images obtained with an electronic endoscope.

Yoichi Miyake

Professor at the Graduate School, Chiba University
Director of the Research Center for Frontier Medical Engineering

Profile

Yoichi Miyake earned his master's degree from the Graduate School, Chiba University in 1968 and received his doctorate in engineering at Tokyo Institute of Technology in 1978. After working as a research assistant and associate professor at Kyoto Institute of Technology and a researcher at the Swiss Federal Institute of Technology (ETH), he was appointed associate professor at Chiba University in 1982, professor in 1989, and director of the Research Center for Frontier Medical Engineering, Chiba University in 2003. He also served as a visiting professor at the Institute of Optics, University of Rochester, professor at Tokyo Institute of Technology (double duty), visiting professor at Chulalongkorn University in Thailand, president of the Society of Photographic Science and Technology of Japan, chief executive of the Japanese Association of Science and Technology for Identification (currently Japanese Association of Forensic Science and Technology), and vice president of the Society for Imaging Science and Technology. He was selected as a fellow and honorary member of the Society for Imaging Science and Technology and received many awards including the Charles E. Ives Award, Electronic Imaging Honoree of the Year (SPIE, IS&T), and honorary award from the Society of Photographic Science and Technology of Japan. He has written many books including Analysis and Evaluation of Digital Color Images (University of Tokyo Press) and Manual of Spectral Image Processing (as an editor and writer, University of Tokyo Press).

Principle of FICE Spectral Estimation Image Processing

1. Introduction

Light we can perceive (visible light) consists of electromagnetic waves with a wavelength of 400 to 700 nm. The light may be separated with a prism or a diffraction grating into red to purple light as shown in Figure 1.

Figure 1. Dispersion of Visible Light with a Prism.

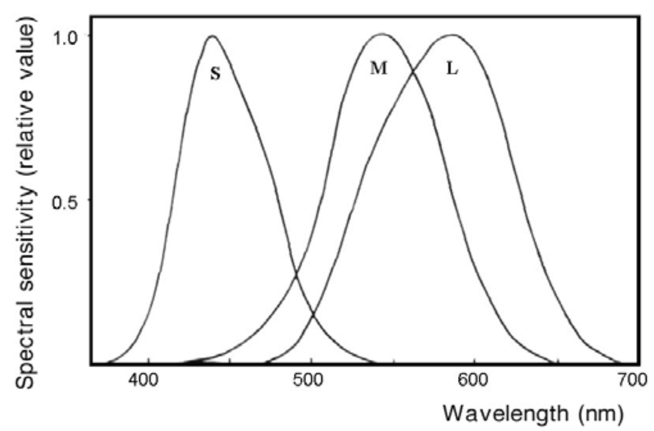

Figure 2. Spectral Sensitivity of L, M, and S Cones (relative value).

When illuminated with visible light as described above, the object reflects some light, which is received by the L, M, or S cone in the retina that is sensitive to red (R), green (G), or blue (B) as shown in Figure 2 and then perceived as color in the cerebrum. Image input systems, such as CCD cameras and color films, use sensors or emulsions sensitive to RGB light to record the colors of the object. Image reproduction is based on the trichromatic theory that is characterized by additive and subtractive color mixing of the primary colors of R, G, and B or cyan (C), magenta (M), and yellow (Y). Briefly, imaging systems, such as a television set, camera, printing machine, copier, and printer, produce color images by integrating spectra in terms of either R, G, and B or C, M, and Y, each of which has a wide bandwidth, and mixing these elements. For example, the use of R, G, and B, each of which has 8 bits or 256 levels of gray scale, will display 2^{24} colors ($256 \times 256 \times 256 = 16.7$ million). The theory for color display and measurement has been organized to establish the CIE-XYZ color system on the basis of the trichromatic theory. Uniform color spaces, such as L*a*b* and L*u*v*, which have been developed from the color system, provide a basis for the development of a variety of imaging systems in the emerging era of multimedia. The development of endoscopes is not an exception, in which CCD-based electronic endoscopes have developed from color film-based recording devices called gastrocameras. However, the quality of color images, particularly reproduced colors, is influenced significantly by the spectral characteristics of imaging devices, as well as illumination and visual environments. Thus, recording and reproduction of spectral information on the object rather than information on three primary colors (RGB) is required in electronic museums, digital archives, electronic commerce, telemedicine, and electronic endoscopy in which recording and reproduction of high-definition color images are necessary. We have been leading the world in developing five-band spectral cameras for digital archiving.[1,2,7] Spectral information includes information on all visible light from the object and may be used for new types of recording, measurement, and diagnosis that cannot be achieved with the three primary colors of RGB or CMY. This chapter outlines the principle of FICE (Flexible spectral Imaging Color Enhancement) , a spectral endoscopic image processing that incorporates such spectral information for the first time.

2. Color Reproduction Theory

Image recording and reproduction aim to accurately record and reproduce the three-dimensional structure and color of an object. Most commonly, however, an object with three-dimensional information is projected onto the two-dimensional plane for subsequent recording, transmission, display, and observation. For color information, three bands of R, G, and B have long been recorded as described above, rather than spectral reflectance. Specifically, colors are reproduced by additive color mixing of the three primary colors of R, G, and B or by subtractive color mixing of the three primary colors of C, M, and Y.

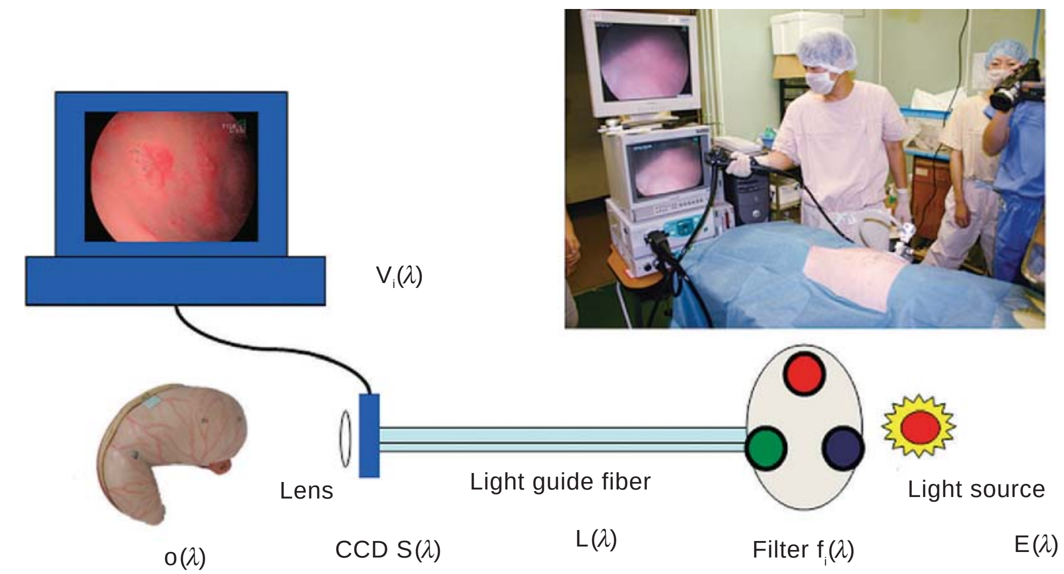

Figure 3. Color Reproduction Process for Electronic endoscopy.

In general, the characteristics of an object can be expressed as the function O (x,y,z,t,λ) of three-dimensional space (x,y,z), time (t), and wavelength (λ) of visible light (400 to 700 nm). More accurate description of object characteristics requires the measurement of the Bidirectional Reflectance Distribution Function(BRDF) of the object. For simplicity, however, this section disregards time, special coordinates, and angle of deviation and focuses on wavelength information of the object O(λ) to address color reproduction in the electronic endoscope as shown in Figure 3. When an object (such as the gastric mucosa) with a spectral reflectance of O(λ) is illuminated with a light source having a spectral emissivity of E(λ) through a filter with a spectral transmittance of $f_i(\lambda)$ (i = R, G, B), and an image obtained through a lens and fiber with a spectral transmittance of L(λ) is recorded with a CCD camera with a spectral sensitivity of S(λ), camera output V_i (i = R, G, B) can be expressed by the equation (1) (for simplicity, noise is ignored).

$$V_i = \int_{400}^{700} E(\lambda)\, f_i(\lambda)\, L(\lambda)\, S(\lambda)\, O(\lambda)\, d\lambda \qquad i=R,G,B \tag{1}$$

Equation (1) can be expressed with a vector as follows:

$$\mathbf{v}_i = \mathbf{f}_i^t \mathbf{ELso} = \mathbf{H}_i^t \mathbf{o} \tag{2}$$

where, $\mathbf{H}_i^t$ is the system's spectral product $\mathbf{f}_i^t\,\mathbf{ELs}$, and t indicates transposition.
This means that the colors reproduced by the endoscope are determined after input of $\mathbf{v}$ into a display, such as a CRT and LCD, and the addition of the characteristics of the display and visual environment. When psychological factors, such as visual characteristics, are disregarded, the colors recorded and displayed with an electronic endoscope are determined by the spectral reflectance of the gastric mucosa (object) and the spectral characteristics of the light source for the illumination and imaging system. Thus, the spectral

reflectance of the gastric mucosa allows the prediction of color reproduction by the endoscope.
In the 1980s, however, there was no report of direct measurement of the spectral reflectance of the gastric mucosa. Thus, we developed an endoscope spectroscopy system to quantitatively investigate color reproduction for endoscopy and measured, for the first time in the world, the spectral reflectance of the gastric mucosa at Toho University Ohashi Medical Center, Cancer Institute Hospital, and the National Kyoto Hospital.[3),(4]

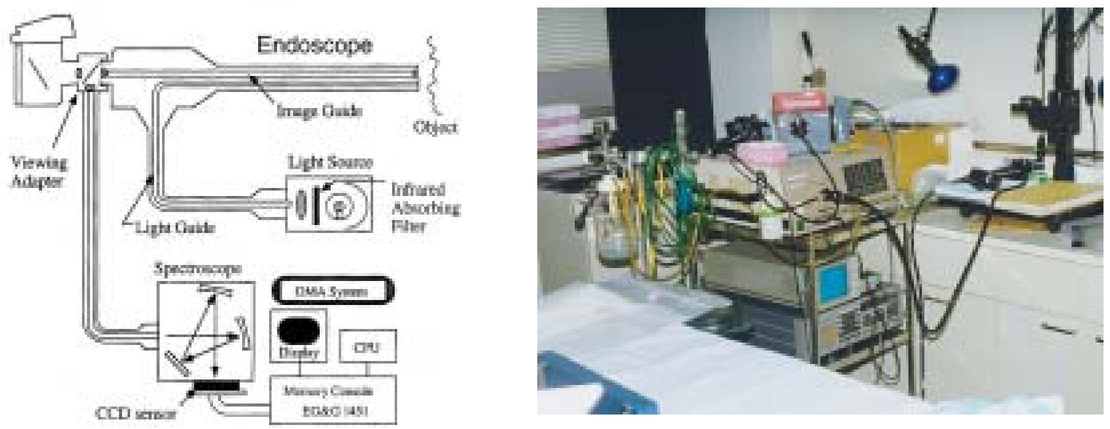

Figure 4. Configuration and Photograph of Endoscope Spectroscopy System.

Figure 4 shows a block diagram and photograph of a spectral endoscope. This spectroscope consists of a light source, optical endoscope, spectroscope, and spectroscopic measurement system (optical multichannel analyzer, or OMA). The object is illuminated with light from the light source through the light guide. Through an image guide and half mirror, the reflected light is delivered partly to the camera and partly to the spectroscope. The luminous flux delivered to the spectroscope has a diameter of 0.24 mm and is presented as a round mark in the eyepiece field. When the distance between the endoscope tip and the object is 20 mm, the mark corresponds to a diameter of 4 mm on the object. A 1024-channel CCD line sensor is placed at the exit pupil of the spectroscope, and the output is transmitted to the PC for analysis. Wavelength calibration was performed with mercury spectrum and a standard white plate. The wavelengths measured range from 450 to 900 nm when an infrared filter is removed from the endoscope.

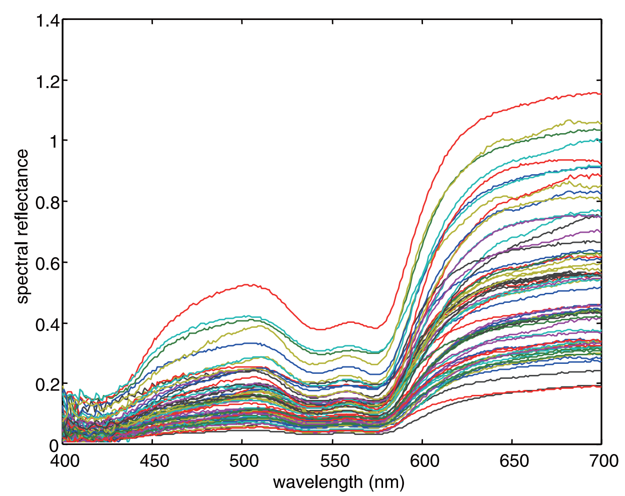

Figure 5. Spectral Reflectance of the Colorectal Mucosa (normal region).

Figure 5 shows an example of the spectral reflectance of normal, colorectal mucosa after denoising and other processing of measurements. As shown in equation (1), the measurement of O(λ) allowed simulation of color reproduction. Initially, I optimized the spectral sensitivity of color films used for the endoscope. However, the measurement of O(λ) represented a single spot on the gastric mucosa. The measurement of the spectral reflectance at all coordinates of the object required huge amounts of time and costs and was not feasible with this spectroscope. Thus, an attempt was made to estimate the spectral reflectance of the gastric mucosa from the camera output.

3. Estimation of Spectral Reflectance

The spectral reflectance of an object may be estimated from the camera output by solving the integral equations (1) and (2). Compared with the camera output, however, the spectral reflectance generally has a greater number of dimensions. For example, the measurement of visible light with a wavelength of 400 to 700 nm at intervals of 5 nm is associated with 61 dimensions. Thus, it is necessary to solve an Ill-posed equation in order to estimate 61 dimensions of spectral information from three-band data (RGB) in conventional endoscopy. This chapter does not detail the problem because a large body of literature is available, and I have also reported it elsewhere.[1),(2] For example, an eigenvector obtained from the principal component analysis of spectral reflectance may be used for estimation as shown in equation (3),

$$\mathbf{o}=\sum_{i=1}^{n}\alpha_i\,\mathbf{u}_i+\mathbf{m} \qquad (3)$$

where **u** is an eigenvector obtained by the principal component analysis of the mucosal spectral reflectance, α is a coefficient calculated from the system spectral product, and **m** is the mean vector.

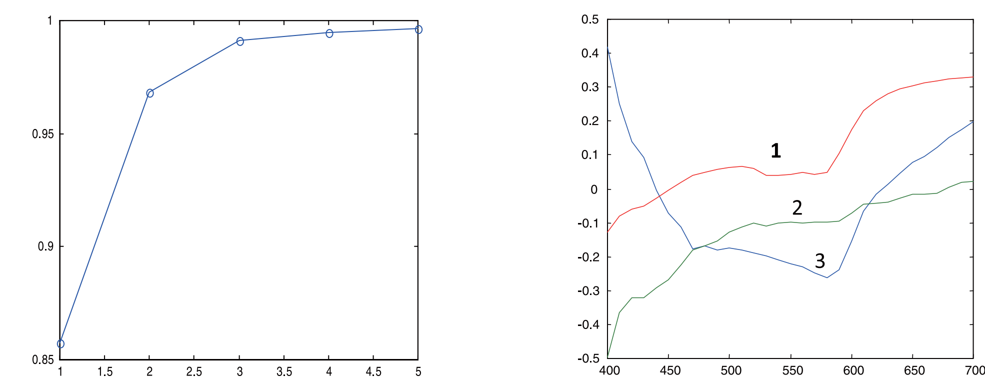

(a) Cumulative Contribution in Estimation of Spectral Reflectance

(b) The First, Second, and Third Principal Components of Spectral Reflectance

Figure 6. Principal Component Analyses of the Spectral Reflectance of the Colorectal Mucosa.

Figure 6 shows the eigenvectors of spectral reflectances of the colorectal mucosa and cumulative contribution. Figure 6 indicates that three principal component vectors allow good estimation of the spectral reflectances of the colorectal mucosa. It was also found that the use of three principal components allowed estimation of the spectral reflectances of the gastric mucosa and skin.[5),(6] For example, when a comparison was made between 310 spectral reflectances estimated from three principal component vectors and those actually measured in the gastric mucosa, the maximum color difference was 9.14, the minimum color difference was 0.64, and the mean color difference was 2.66. These findings indicated that output of a three-channel camera allowed estimation of the spectral reflectance with satisfactory accuracy.
When the system spectral product is not known, the Wiener estimation may be used to estimate the spectral reflectance of an object.[7),(8] This section briefly describes the estimation of the spectral reflectance by the Wiener estimation. The pseudo-inverse matrix $\mathbf{H}^{-1}$ of the system matrix should be computed to obtain **o** from the equation (2). For determination of the estimation matrix, an endoscope is used to capture sample color charts corresponding to spectral radiance **o** as shown in Figure 7, and the camera output **v** should be measured. In this case, the estimate of spectral radiance of sample k can be expressed with the camera output as shown below.

Figure 7. Measurement of the Spectral Reflectance by the Wiener Estimation.

$$\mathbf{o}'_k = \mathbf{H}^{-1}\mathbf{v}_k \qquad (4)$$

According to the Wiener estimation method, the pseudo-inverse matrix that minimizes the error between the actual spectral radiance $\mathbf{o}_k$ and the estimate $\mathbf{o}'_k$ $<|\mathbf{o}'_k - \mathbf{o}_k|>$ for all sample data can be obtained from the following equation,

$$\mathbf{H}^{-1} = \mathbf{R}_{fg}\mathbf{R}_{gg}^{-1} \qquad (5)$$

where $\mathbf{R}_{fg}$ is a correlation matrix for the spectral radiance and camera output, and $\mathbf{R}_{gg}$ is an auto-correlation matrix for the camera output. In FICE,[9,10] the spectral reflectance of an object is determined on the basis of the Wiener estimation.

4. Spectral Image

Figure 8 schematically shows the spectral estimation and image reconstruction based on the principle.

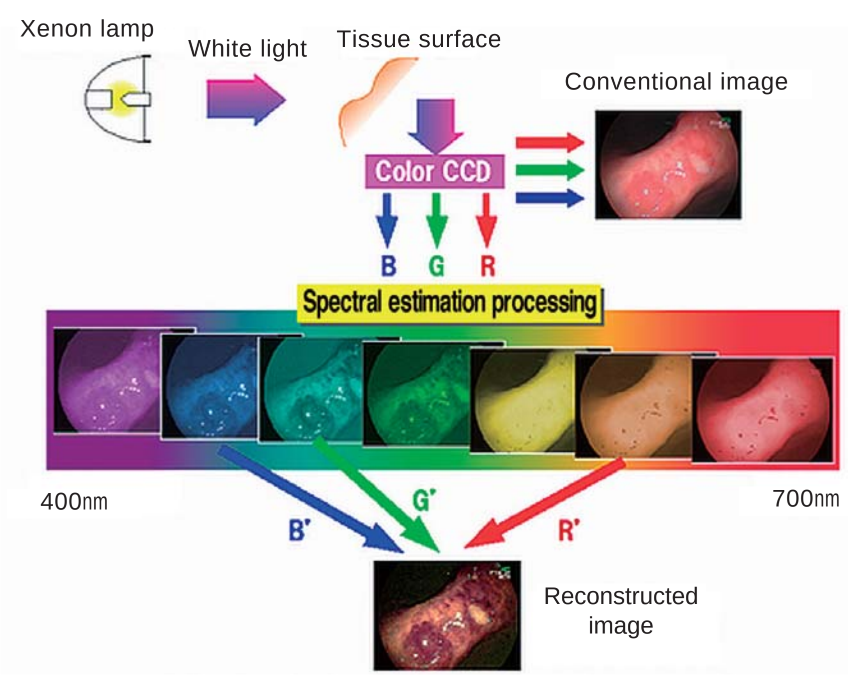

Figure 8. Method for Image Construction Using Spectral Estimation

Figure 9 shows examples of spectral images at (a) 400 nm, (b) 450 nm, (c) 500 nm, (d) 550 nm, (e) 600 nm, (f) 650 nm, and (g) 700 nm estimated from an RGB image (h) of the gastric mucosa.

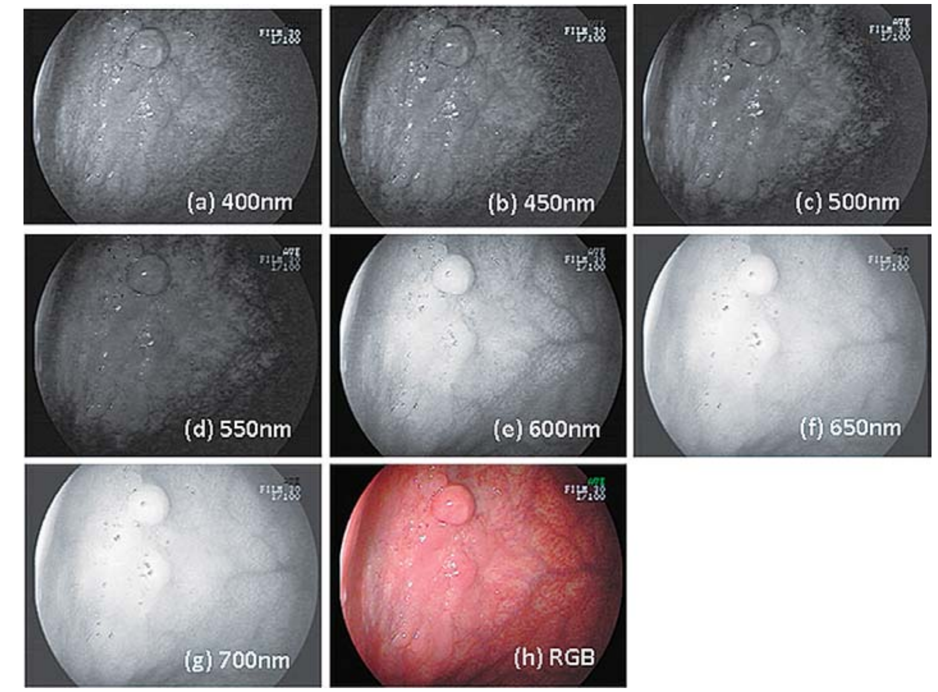

Figure 9. Examples of Spectral Images at 400 to 700 nm Estimated From an RGB Image of the Gastric Mucosa.

FICE has pre-calculated coefficients in a look-up table and estimates images at three wavelengths (λ_1, λ_2, λ_3) , or spectral images, by using the following 3 × 3 matrix.

$$\begin{bmatrix} \lambda_1 \\ \lambda_2 \\ \lambda_3 \end{bmatrix} = \begin{bmatrix} k_{1r} & k_{1g} & k_{1b} \\ k_{2r} & k_{2g} & k_{2b} \\ k_{3r} & k_{3g} & k_{3b} \end{bmatrix} \begin{bmatrix} R \\ G \\ B \end{bmatrix} \qquad (6)$$

For example, the matrix coefficients for determination of wavelengths (λ_1 = 500 nm, λ_2 = 620 nm, λ_3 = 650 nm) are as follows:

$$\begin{bmatrix} \lambda_1 \\ \lambda_2 \\ \lambda_3 \end{bmatrix} = \begin{bmatrix} -0.00119 & 0.002346 & 0.0016 \\ 0.004022 & 0.000068 & -0.00097 \\ 0.005152 & -0.00192 & 0.000088 \end{bmatrix} \begin{bmatrix} R \\ G \\ B \end{bmatrix} \qquad (7)$$

Thus, FICE assigns estimated spectral images to RGB components in a display device and allows reproduction of color images at a given set of wavelengths in real time. Figure 10 shows a FICE block diagram.

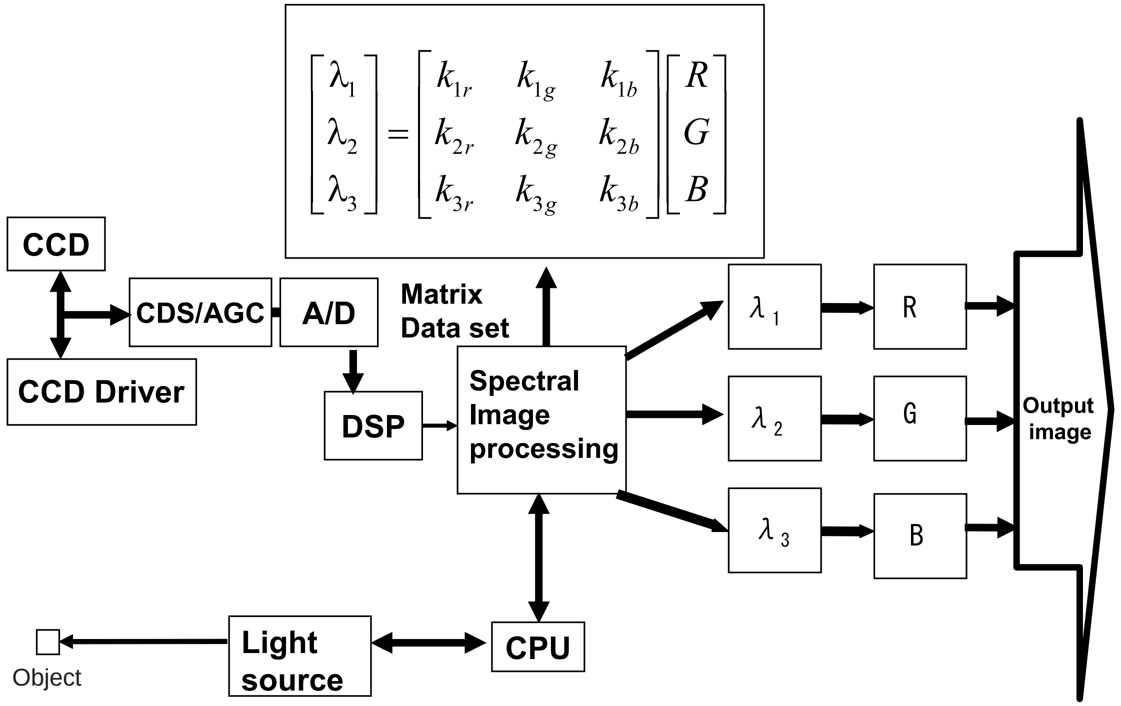

Figure 10. FICE Block Diagram.

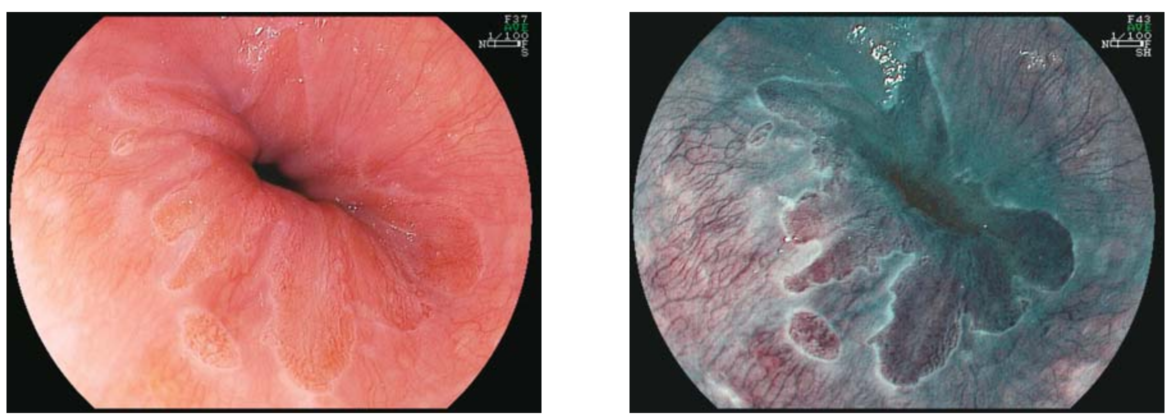

(a) RGB image (Conventional Image)

(b) FICE image (R: $\lambda 1$ = 500nm, G: $\lambda 2$ = 450nm, B: $\lambda 3$ = 410nm)

Figure 11. Esophageal mucosa visualized by FICE.
(Images provided by Dr. Kouzu, Chiba University)

Figure 11 shows an example of an endoscopic image of the esophagus taken with this endoscopy system. Figure (a) shows an image produced with conventional RGB data, and Figure (b) shows an example of an image in which RGB components are replaced with spectral components (R, 500 nm; G, 450 nm; B, 410 nm). In Figure (b) blood vessels and the contours of inflammatory tissue associated with reflux esophagitis are highlighted.

(a)

(b)

(c)

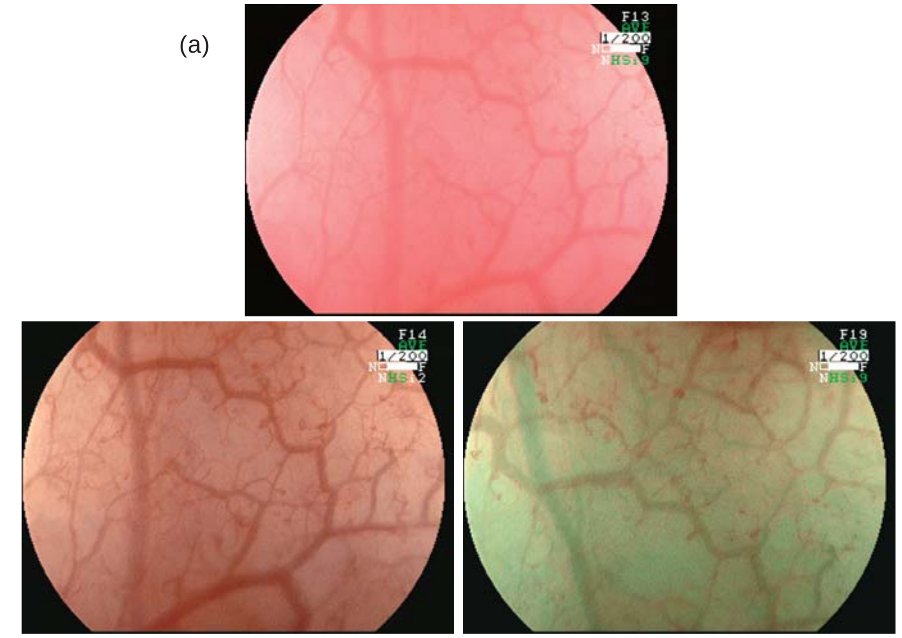

(a) RGB image (conventional image)
(b) FICE image (R, 550 nm; G, 500 nm; B, 470 nm)
(c) FICE image (R, 550 nm; G, 500 nm, B, 400 nm)

Figure 12. Images of lower esophageal mucosa
(Images provided by Dr. Inoue, Chiba University)

Figure 12 shows images of the mucosa of the lower esophagus in which different combinations of wavelengths result in different color reproductions. Figure (a) shows an image reproduced with the conventional RGB data, and Figure (b) shows an image reproduced with spectra (R, 550 nm; G, 500 nm; B, 470 nm) and Figure (c) shows an image reproduced with spectra (R, 550 nm; G, 500 nm; B, 400 nm). Thus, the FICE endoscope produces images of an object with given wavelengths, thereby enhancing the appearance of mucosal tissue variations. Unlike processing with narrow-band optical filters, this system allows the combination of a huge number of observation wavelengths and rapid switching of the wavelengths using a keyboard. The system also allows switching between conventional and spectral images with the push of a button on the endoscope, providing the physician fingertip control, enabling simple and convenient enhancement of diagnostic procedures.

Figure 13. Photograph of Endoscopy System Incorporating FICE Function.

5. Summary

This chapter outlined the principle of FICE spectral image processing for endoscopy using the Fujinon VP-4400 video processor. FICE was commercialized by combining basic research, development of the endoscope spectroscopy system, measurement of the spectral reflectance of the gastrointestinal mucosa, principal component analysis of the spectral reflectance, and the Weiner estimation method. Ongoing development will realize even better systems in the future with more powerful capabilities and unleashing the full potential of spectral image enhancement.

[References]
Images contained in this atlas use the below convention to signify the application of FICE settings.
(1) Miyake Y. Analysis and Evaluation of Digital Color Images. University of Tokyo Press; 2000.
(2) Miyake Y, editor. Manual of Spectral Image Processing. University of Tokyo Press; 2006.
(3) Miyake Y, Sekiya T, Kubo S, Hara T. A new spectrophotometer for measuring the spectral reflectance of gastric mucous membrane. J. Photographic Science. 1989;37:134-138.
(4) Sekiya T, Miyake Y, Hara T. Measurement of the spectral reflectance of gastric mucous membrane and color reproduction simulation for endoscopic images. Kyoto University Publications of the Research Institute for Mathematical Sciences. 1990;736:101-130.
(5) Shiobara T, Haneishi H, Miyake Y. Color correction for colorimetric color reproduction in an electronic endoscope. Optics Communications. 1995;114:57-63.
(6) Shiobara T, Zhou S, Haneishi H, Tsumura N, Miyake Y. Improved color reproduction of electronic endoscopes. J. Imaging Science and Technology. 1996;40(6):494-501.
(7) Miyake Y, Yokoyama Y. Obtaining and reproduction of accurate color images based on human perception. Proc. SPIE3300. 1998;190-197.
(8) Tsumura N, Tanaka T, Haneishi H, Miyake Y. Optimal design of mosaic color electronic endoscopes. Optics Communications. 1998;145:27-32.
(9) Miyake Y, Kouzu T, Takeuchi S, Nakaguchi T, Tsumura N, Yamataka S. Development of new electronic endoscopes using the spectral images of an internal organ. Proc. 13th CIC13, 261-263 (Scottsdale, 2005).
(10) Miyake Y, Kouzu T, Yamataka S. Development of a spectral endoscope. Image Lab. 2006;17:70-74.

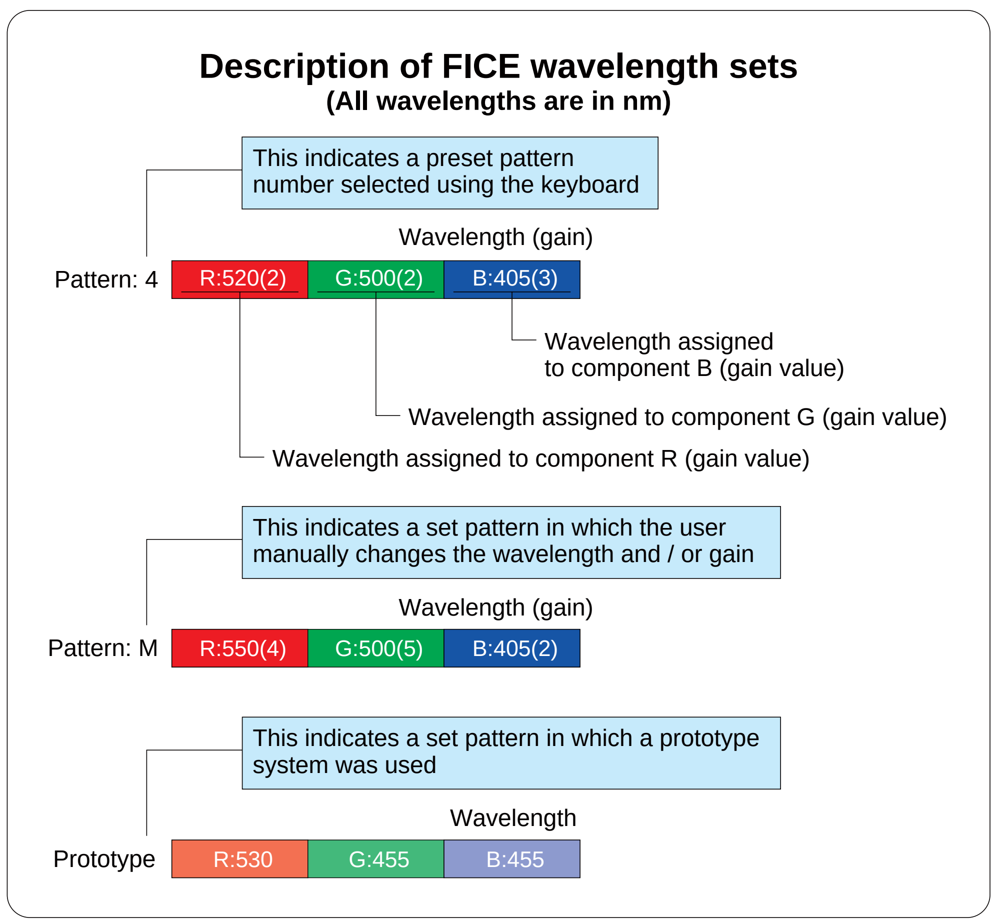

Examination of the Boundary and Area using FICE

This chapter presents cases in which the boundary between diseased and normal regions and individual areas are clearly visualized with the use of FICE.

Examination of the Boundary and Area using FICE

Esophagus

Conventional image

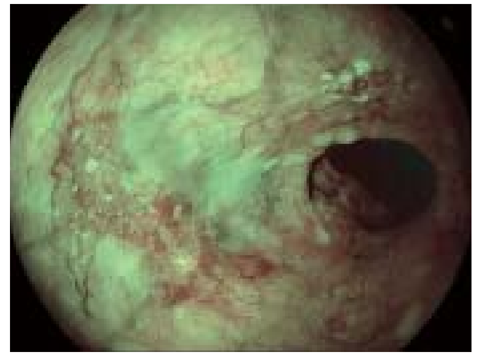

Wavelength

Prototype R:530 G:455 B:455

Site : Esophagus

Case : SCC, 0-IIc, m1

Findings : In a pale erythematous site seen by conventional examination, the use of FICE allows clearer visualization of the boundary.

Photographs provided by Dr. Yoshida (Hiroshima University)

Esophagus

Conventional image

Wavelength

Prototype R:530 G:455 B:455

Iodine staining image

Site : Esophagus

Case : SCC, 0-IIc, m1

Findings : In a pale erythematous area on the conventional image, the use of FICE allows clearer visualization of the boundary of the lesion and easy identification of the area.

Photographs provided by Dr. Yoshida (Hiroshima University)

Esophagus

Conventional image

Wavelength

Prototype R:530 G:455 B:455

Site : Esophagus

Case : SCC, 0-IIc, m1

Findings : Compared with conventional examination, the use of FICE highlights color changes in the affected area.

Photographs provided by Dr. Yoshida (Hiroshima University)

Esophagus

Conventional image

Wavelength (gain)

Pattern: M R:525(4) G:495(3) B:495(1)

Site : Esophagus

Case : IIc lesion in the middle esophagus

Findings : Case in which the boundary of esophageal cancer is clearly observed. FICE allows clear visualization of the boundary and identification of the obstruction of blood vessels.

Photographs provided by Dr. Kouzu (Chiba University)

Boundary
Vasculature
Magnifying
Vasculature and Magnification
Pathological
Enteroscopy
Transnasal

Examination of the Boundary and Area using FICE

Stomach

Conventional image

Wavelength

Prototype R:530 G:455 B:455

Site : Stomach

Case : 0-IIc, moderately differentiated tubular adenocarcinoma

Findings : Compared with conventional examination, FICE allows clear visualization of the area of the lesion.

Photographs provided by Dr. Yoshida (Hiroshima University)

Stomach

Conventional image

Wavelength (gain)

Pattern: M R:550(2) G:500(5) B:470(4)

Site : Stomach

Case : Early gastric cancer, 0-IIa, well-differentiated adenocarcinoma

Findings : An elevated lesion is found in the lesser curvature of the mid body, leading to the diagnosis of early gastric cancer. On the FICE image, the demarcation line between the elevated lesion and the surrounding area is clearly visualized.

Photographs provided by Dr. Osawa and Dr. Yoshizawa (Jichi Medical University)

Stomach

Conventional image

Wavelength (gain)

Pattern: M R:550(2) G:500(5) B:470(4)

Site : Stomach

Case : Early gastric cancer, 0-IIc, Signet ring cell carcinoma

Findings : On the FICE images, the whitish color change is enhanced in the edge of depressed area, and thereby the lesion is clearly visualized.

Photographs provided by Dr. Osawa and Dr. Yoshizawa (Jichi Medical University)

Stomach

Conventional image

Wavelength (gain)

Pattern: M R:550(2) G:500(5) B:470(4)

Site : Stomach

Case : Early gastric cancer, 0-IIc, well-differentiated adenocarcinoma

Findings : On the conventional endoscopic image, a reddish depressed lesion is found in the lesser curvature of the mid body. On the FICE image, the surrounding atrophic mucosa turns yellowish. Thus, reddish cancerous lesion is enhanced and the edge of depressed lesion is clearly visualized.

Photographs provided by Dr. Osawa and Dr. Yoshizawa (Jichi Medical University)

Boundary
Vasculature
Magnifying
Vasculature and Magnification
Pathological
Enteroscopy
Transnasal

Examination of the Boundary and Area using FICE

Stomach

Conventional image

Wavelength (gain)

Pattern: M R:550(2) G:500(5) B:470(4)

Site : Stomach
Case : Early gastric cancer, 0-IIa, Cancer in adenoma, well-differentiated adenocarcinoma.
Findings : On the conventional endoscopic image, slightly elevated lesion is found on the posterior wall of the mid body. On the FICE image, the whitish change of the elevated lesion is more evident, and a long pit pattern of adenomatous portion in the edge of elevated area and a fine pit pattern of cancerous portion are clearly observed with low magnification.

Photographs provided by Dr. Osawa and Dr. Yoshizawa (Jichi Medical University)

Stomach

Conventional image

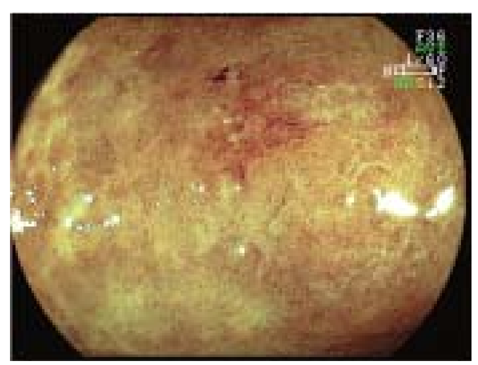

Wavelength (gain)

Pattern: M R:550(2) G:500(5) B:470(4)

Site : Stomach
Case : Early gastric cancer, 0-IIc, well-differentiated adenocarcinoma
Findings : On the conventional endoscopic image, slightly irregular surface mucosa is found in the lesser curvature of the mid body. On the FICE image, the lesion is visualized as a reddish depressed area, and the demarcation line between the cancerous portion and the surrounding area is clearly observed.

Photographs provided by Dr. Osawa and Dr. Yoshizawa (Jichi Medical University)

Stomach

Conventional image

Wavelength (gain)

Pattern: M R:550(2) G:500(5) B:470(4)

Conventional image

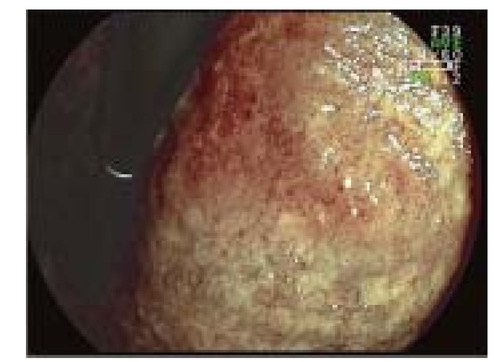

Wavelength (gain)

Pattern: M R:550(2) G:500(5) B:470(4)

Site : Stomach
Case : Early gastric cancer, 0-IIc, well-differentiated adenocarcinoma
Findings : On the conventional endoscopic image, mild reddish mucosa is found in the lesser curvature of the upper body. On the FICE image, the surrounding area turns yellowish and a reddish area with slightly depressed cancer is clearly delineated.

Photographs provided by Dr. Osawa and Dr. Yoshizawa (Jichi Medical University)

Boundary
Vasculature
Magnifying
Vasculature and Magnification
Pathological
Enteroscopy
Transnasal

Examination of the Boundary and Area using FICE

Stomach

Conventional image

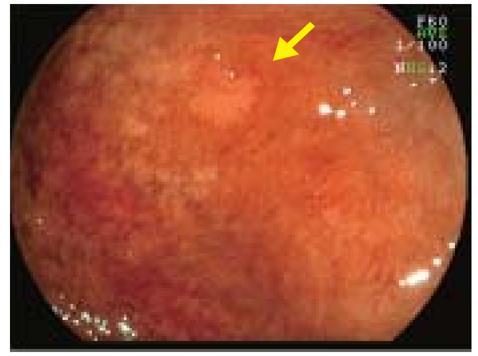

Wavelength (gain)

Pattern: 2 R:550(2) G:500(2) B:470(3)

Site : Anterior wall of the lower body of the stomach

Case : Early gastric cancer, IIb

Findings : The lesion characterized only by a slight color change is hardly identifiable under white light but distinguishable by FICE. A pathological diagnosis of well-differentiated adenocarcinoma is made.

Photographs provided by Dr. Inoue (Chiba University)

Stomach

Conventional image

Wavelength (gain)

Pattern: 4 R:520(2) G:500(2) B:405(3)

Site : Lesser curvature of the body of the stomach

Case : Early gastric cancer (IIa + IIc)

Findings : FICE clearly visualizes the depressed area as well as the appearance and boundary of the surrounding elevated area. A pathological diagnosis of moderately differentiated adenocarcinoma is made.

Photographs provided by Dr. Inoue (Chiba University)

Stomach

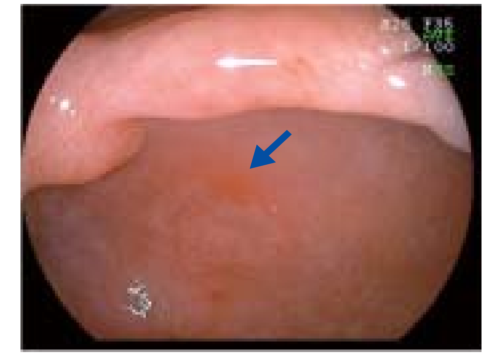

Conventional image

Wavelength (gain)

Pattern: M R:525(4) G:495(3) B:495(1)

Site : Gastric antrum

Case : IIc + IIb adenocarcinoma

Findings : In the caudal side of the scar related to EMR, the malignant lesion is clearly visualized by FICE.

Photographs provided by Dr. Kouzu (Chiba University)

Stomach

Conventional image

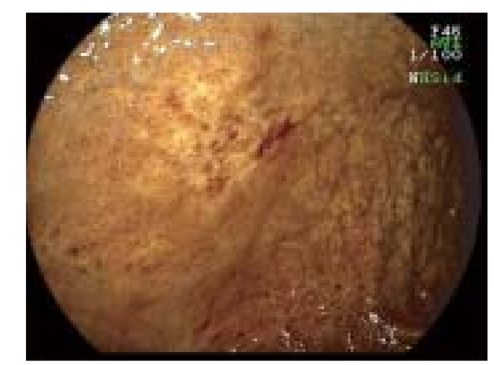

Wavelength (gain)

Pattern: M R:525(4) G:495(3) B:495(1)

Site : Gastric corpus

Case : IIc adenocarcinoma

Findings : Discolored lesion in the anterior wall of the gastric corpus. A case of cancer in which microvessels on the surface are observed by FICE.

Photographs provided by Dr. Kouzu (Chiba University)

Examination of the Boundary and Area using FICE

Stomach

Conventional image

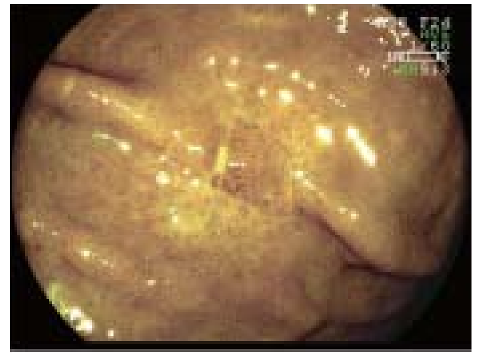

Wavelength

Prototype	R:550	G:500	B:400

Site : Stomach

Case : Early gastric cancer, 0-IIc, signet-ring cell carcinoma

Findings : Early gastric cancer, superficial depressed type, in the greater curvature of the upper body of the stomach. The poorly defined, discolored area on conventional view is clearly visualized by FICE.

Photographs provided by Dr. Mitsufuji (Kyoto Prefectural University of Medicine)

Stomach

Conventional image

Wavelength

Prototype	R:540	G:415	B:415

Site : Stomach

Case : Early gastric cancer, 0-IIc, well-differentiated adenocarcinoma (tub1 > tub2), 11 × 7mm in size

Findings : The conventional image shows an ill-defined slightly depressed reddish lesion in the anterior wall of the upper body of the stomach. On the FICE image, the border of the cancerous lesion is well demarcated.

Photographs provided by Dr. Mitsufuji (Kyoto Prefectural University of Medicine)

Stomach

Conventional image

Wavelength (gain)

Pattern: 4	R:520(2)	G:500(2)	B:405(3)

Site : Stomach

Case : Gastric adenoma

Findings : The boundary of the lesion that is hardly identifiable by conventional examination is clearly visualized by FICE.

Photographs provided by Dr. Inoue (Chiba University)

Stomach

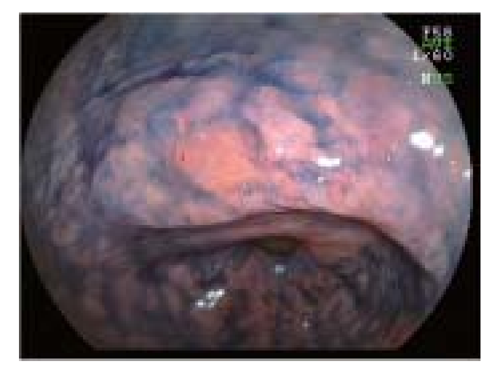

FICE image without indigo carmine

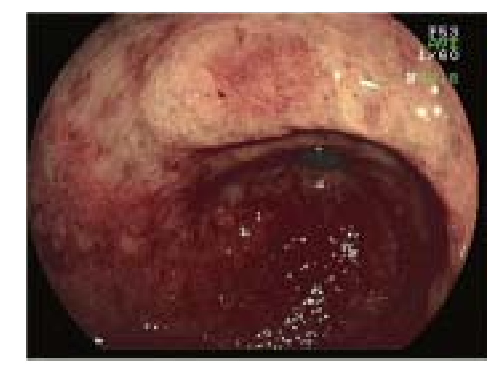

Wavelength (gain)

Pattern: M	R:525(4)	G:495(4)	B:495(3)

Site : Stomach

Case : Gastric adenoma with a slightly depressed area on the top

Findings : The boundary between the elevated and depressed areas is clearly visualized by highlighting the color changes.

Photographs provided by Dr. Inoue (Chiba University)

Boundary
Vasculature
Magnifying
Vasculature and Magnification
Pathological
Enteroscopy
Transnasal

Examination of the Boundary and Area using FICE

Stomach

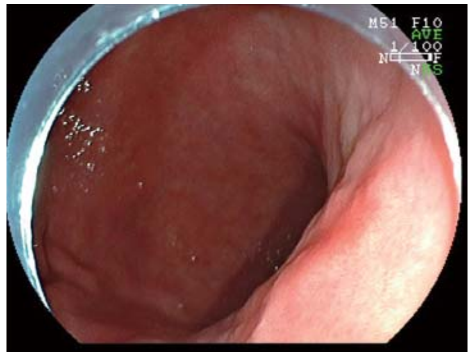

Conventional image

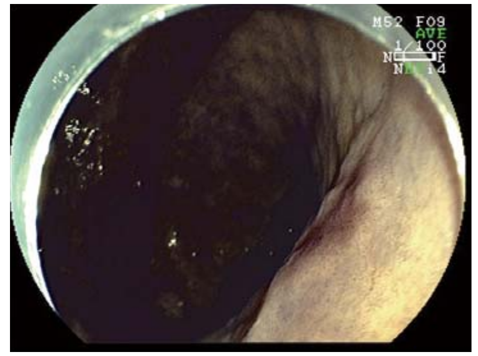

Wavelength (gain)

Pattern: 4 R:520(2) G:500(2) B:405(3)

Site : Stomach

Case : Adenocarcinoma

Findings : A case in which the area of IIc + IIa lesion in the posterior wall of the gastric corpus is clearly visualized.

After EMR, a histological diagnosis of well differentiated tubular adenocarcinoma was made.

Photographs provided by Dr. Kouzu (Chiba University)

Stomach

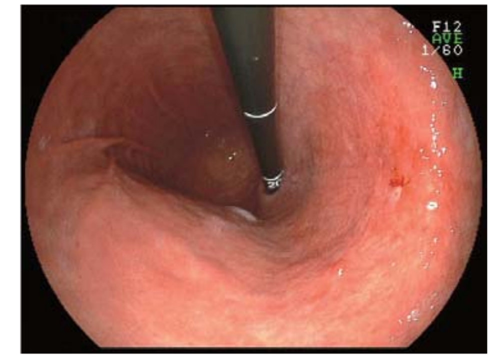

Conventional image

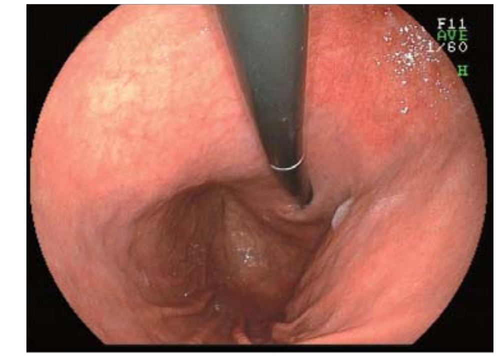

Conventional image

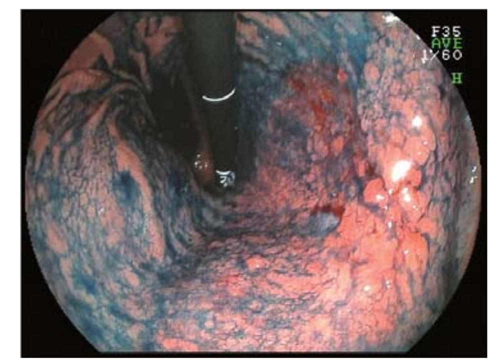

Image after indigo carmine spraying

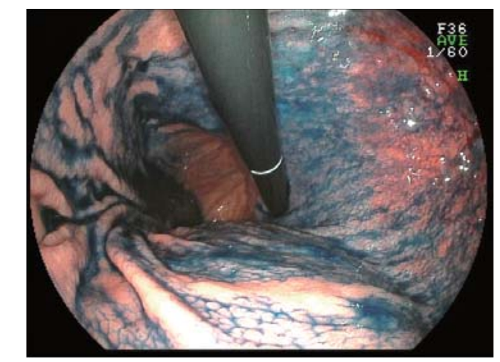

Image after indigo carmine spraying

Wavelength

Prototype R:560 G:500 B:475

Wavelength

Prototype R:560 G:500 B:475

Site : Stomach

Case : Early gastric cancer, 0-IIa + IIb

Findings : The FICE image displays not only superficial elevated lesion (type 0-IIa) but also flat lesion (0-IIb) extensively involving the lesser curvature of the gastric body. Its boundary is more clearly visualized by FICE than by indigo carmine spraying.

Photographs provided by Dr. Mitsufuji (Kyoto Prefectural University of Medicine)

Examination of the Boundary and Area using FICE

Stomach

Conventional image

Wavelength
Prototype R:555 G:500 B:445

Image after indigo carmine spraying

Wavelength
Prototype R:550 G:500 B:470

Site : Stomach

Case : Early gastric cancer, 0-IIa

Findings : Discolored, elevated lesion in the greater curvature of the gastric remnant. Because of FICE enhancement of color contrast, the boundary between the affected area and the background mucosa is clearly visualized.

Photographs provided by Dr. Mitsufuji (Kyoto Prefectural University of Medicine)

Stomach

Conventional image

Wavelength
Prototype R:540 G:415 B:415

Wavelength
Prototype R:540 G:500 B:445

Wavelength
Prototype R:550 G:500 B:470

Site : Stomach

Case : Early gastric cancer, 0-IIc, signet-ring cell carcinoma

Findings : FICE highlights the reddish depressed area which is consistent with the area of signet-ring cell infiltration. The emphasis of the cancerous lesion helps to determine the bounds of resection by endoscopic submucosal dissection.

Photographs provided by Dr. Mitsufuji (Kyoto Prefectural University of Medicine)

Boundary
Vasculature
Magnifying
Vasculature and Magnification
Pathological
Enteroscopy
Transnasal

Examination of the Boundary and Area using FICE

Stomach

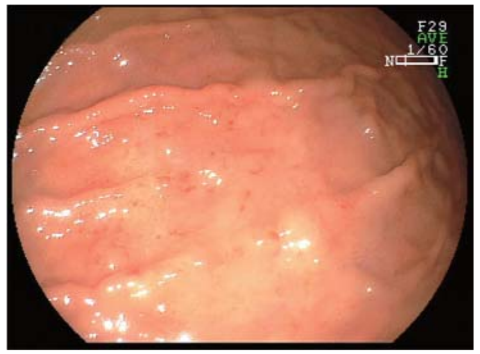

Conventional image

Wavelength

Prototype R:560 G:500 B:475

Wavelength

Prototype R:550 G:500 B:470

Wavelength

Prototype R:540 G:500 B:445

Site : Stomach

Case : MALT lymphoma

Findings : MALT lymphoma in the greater curvature of the gastric body. FICE enhancement of color contrast makes the boundary between the affected area and the background mucosa more clear.

Photographs provided by Dr. Mitsufuji (Kyoto Prefectural University of Medicine)

Observation of Vasculature using FICE

This chapter presents cases in which the use of FICE improves the visibility of vasculature.

Observation of Vasculature using FICE

Esophagus

Conventional image

Wavelength (gain)

Pattern: 4 R:520(2) G:500(2) B:405(3)

Site : Esophagus

Case : Normal esophageal mucosa

Findings : The deep and superficial vascular patterns are more clearly visualized.

Photographs provided by Dr. Inoue (Chiba University)

Esophagus

Conventional magnified image

Wavelength

Prototype R:520 G:500 B:405

Site : Esophagus

Case : SCC, 0-IIc, m1

Findings : In magnifying endoscopy, the use of FICE allows clear visualization of destructed, thread-like microvessels and easy identification of the vascular pattern.

Photographs provided by Dr. Yoshida (Hiroshima University)

Esophagus

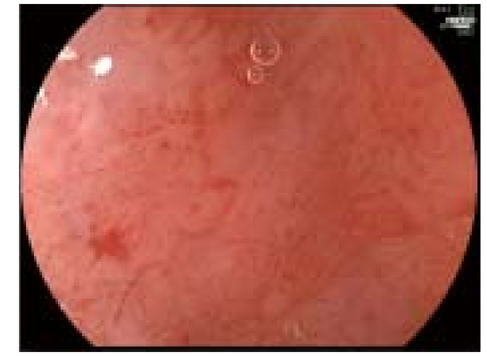

Conventional magnified image

Wavelength

Prototype R:520 G:500 B:405

Site : Esophagus

Case : SCC, 0-IIc, m1

Findings : In magnifying endoscopy, FICE clearly visualizes irregularly arranged microvessels and improves the visibility.

Photographs provided by Dr. Yoshida (Hiroshima University)

Esophagus

Conventional magnified image

Wavelength

Prototype R:520 G:500 B:405

Site : Esophagus

Case : SCC, 0-IIc, m1

Findings : In magnifying endoscopy, the use of FICE allows clear visualization of microvessels.

Photographs provided by Dr. Yoshida (Hiroshima University)

Observation of Vasculature using FICE

Stomach

Conventional magnified image

Wavelength

Prototype R:520 G:500 B:405

Site : Stomach

Case : 0-IIc, well differentiated adenocarcinoma

Findings : In magnifying endoscopy, FICE allows clear visualization of tumor vessels.

Photographs provided by Dr. Yoshida (Hiroshima University)

Stomach

Conventional image

Wavelength (gain)

Pattern: M R:550(2) G:500(5) B:470(4)

Site : Stomach

Case : Gastric antral vascular ectasia (GAVE)

Findings : Telangiectasia in the gastric antrum. Compared with the conventional endoscopic image, dilated capillaries are enhanced with good contrast in the FICE image.

Photographs provided by Dr. Osawa and Dr. Yoshizawa (Jichi Medical University)

Stomach

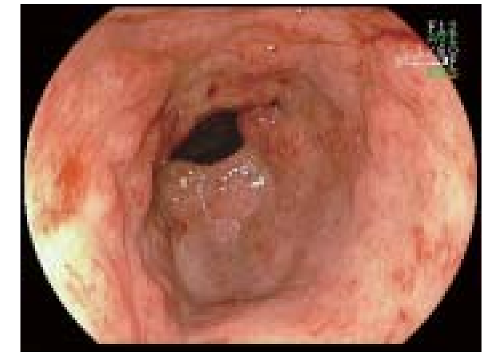

Conventional image

Wavelength (gain)

Pattern: M R:550(2) G:500(5) B:470(4)

Site : Stomach

Case : Gastric antral vascular ectasia (GAVE)

Findings : This case describes a patient with telangiectasia in the gastric antrum who had hematemesis and presented to hospital. Compared with the conventional endoscopic image, dilated capillaries are highlighted with good contrast in the FICE image.

Photographs provided by Dr. Osawa and Dr. Yoshizawa (Jichi Medical University)

Stomach

Wavelength

Prototype R:540 G:415 B:415

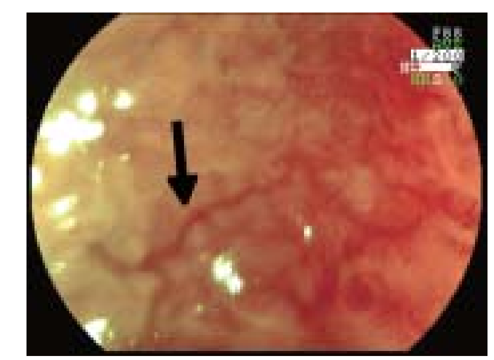

Wavelength

Prototype R:540 G:415 B:415

Site : Stomach

Case : Early gastric cancer, 0-IIc, sm microinvasive carcinoma (150 μm)

Findings : At low magnification (left), the mucosal pit pattern of cancerous area is irregular, and the boundary between the affected area and the background mucosa is clearly visualized. At high magnification (right), cappillary networks are visible, and an abnormal large blood vessel that is distinct from the surrounding fine vessels are detected (arrow).

Photographs provided by Dr. Mitsufuji (Kyoto Prefectural University of Medicine)

Observation of Vasculature using FICE

Large intestine

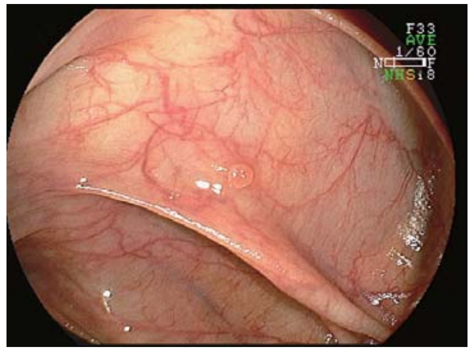

Conventional image

Wavelength

Prototype | R:540 | G:490 | B:420

Site : Large intestine

Case : Normal mucosa

Findings : The vasculature in normal mucosa is clearly visible, and a small polyp is easily identifiable.

Photographs provided by Dr. Togashi (Jichi Medical University)

Large intestine

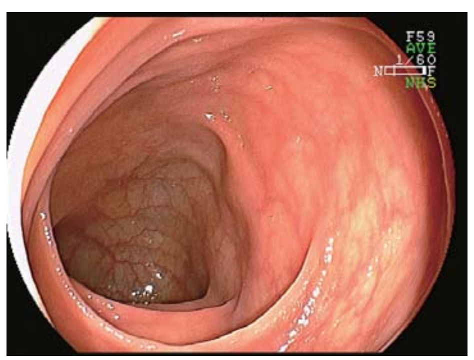

Conventional image

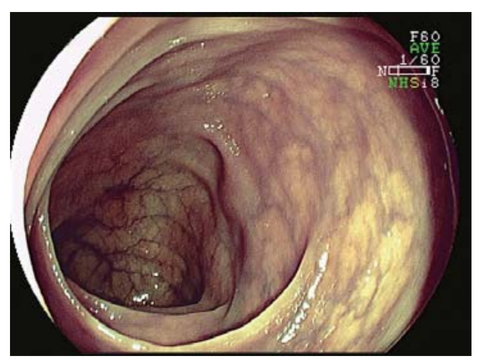

Wavelength

Prototype | R:540 | G:490 | B:420

Site : Large intestine

Case : Normal mucosa

Findings : The vascular pattern in the distal portion is also clearly visualized.

Photographs provided by Dr. Togashi (Jichi Medical University)

Large intestine

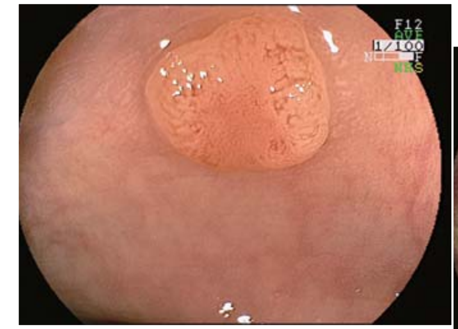

Conventional image

Wavelength

Prototype | R:540 | G:490 | B:420

Image after indigo carmine spraying

Site : Large intestine

Case : Adenoma

Findings : The vascular pattern is visible to some extent on the conventional low-magnified image. Visualization of smaller vessels is, furthermore, enhanced on the FICE image.

Photographs provided by Dr. Togashi (Jichi Medical University)

Large intestine

Conventional image

Wavelength

Prototype | R:540 | G:490 | B:420

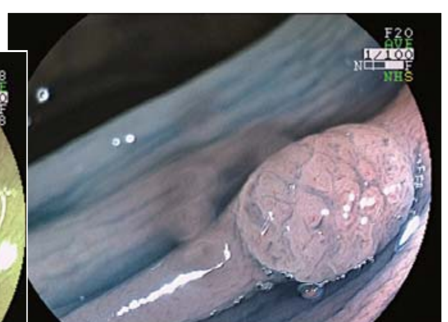

Image after indigo carmine spraying

Site : Large intestine

Case : Adenoma

Findings : The vascular pattern of the polyp is unclear on the conventional low-magnified image but clearly visualized on the FICE image.

Photographs provided by Dr. Togashi (Jichi Medical University)

Boundary
Vasculature
Magnifying
Vasculature and Magnification
Pathological
Enteroscopy
Transnasal

Observation of Vasculature using FICE

Large intestine

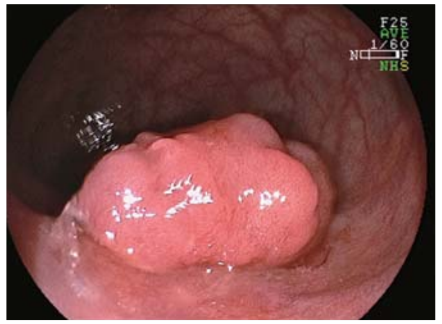
Conventional image

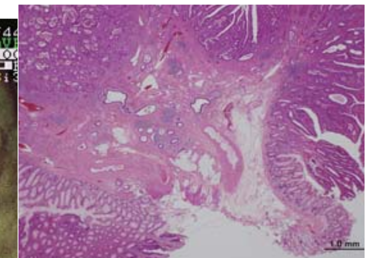
Histopathological image

Wavelength
Prototype R:540 G:490 B:420

Site : Large intestine

Case : Moderately differentiated adenocarcinoma (3500 µm of invasion)

Findings : On the FICE image, the vascular pattern on the surface of the lesion is clearly visualized. Irregular vascular dilatation suggests submucosal, highly invasive carcinoma.

Photographs provided by Dr. Togashi (Jichi Medical University)

Large intestine


Conventional magnified image

Wavelength
Prototype R:540 G:500 B:445

Site : Large intestine (sigmoid colon)

Case : Early colon cancer, carcinoma in adenoma

Findings : Is + IIc lesion in the sigmoid colon. FICE clearly visualizes tortuous, abnormal blood vessels around the tumor and disrupted vascular network in the depressed area. The lesion is found to be carcinoma in adenoma invading the submucosal layer (1200 µm).

Photographs provided by Dr. Mitsufuji (Kyoto Prefectural University of Medicine)

Magnifying Endoscopy with FICE

This chapter presents cases in which the combination of magnifying endoscopy and FICE improves the visibility of pit and microvascular patterns.

Magnifying Endoscopy with FICE

Boundary
Vasculature
Magnifying
Vasculature and Magnification
Pathological
Enteroscopy
Transnasal

Esophagus

Conventional magnified image

Wavelength (gain)

Pattern: M R:525(4) G:495(4) B:495(3)

Site : Esophagus

Case : Early esophageal cancer, IIc

Findings : The appearance of intra-epithelial papillary capillary loops is more clearly visualized.

Photographs provided by Dr. Inoue (Chiba University)

Esophagus

Conventional image

Wavelength (gain)

Pattern: 6 R:580(2) G:520(2) B:460(3)

Site : Esophagus

Case : Early esophageal cancer, IIc

Findings : The appearance of intra-epithelial papillary capillary loops is more clearly visualized. The contrast between the loops and deep vessels is enhanced.

Photographs provided by Dr. Inoue (Chiba University)

Stomach

Conventional magnified image

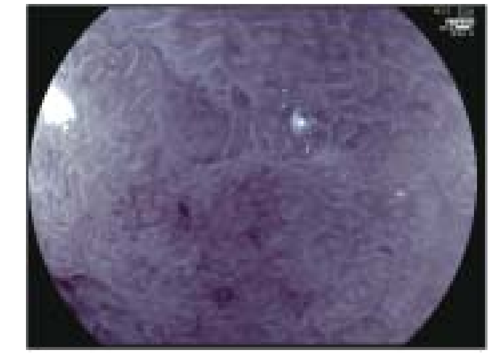

Wavelength

Prototype R:520 G:500 B:405

Site : Stomach

Case : 0-IIc moderately differentiated tubular adenocarcinoma

Findings : In magnifying endoscopy, the use of FICE clearly visualizes microvessels and surface microstructure.

Photographs provided by Dr. Yoshida (Hiroshima University)

Stomach

Conventional magnified image

Wavelength (gain)

Pattern: M R:550(2) G:500(5) B:470(4)

Site : Stomach

Case : Gastric ulcer

Findings : Compared with the conventional endoscopic image, the reddish change of regenerated epithelium is more evident and the ulcer edge is more clearly visualized on the FICE image.

Photographs provided by Dr. Osawa and Dr. Yoshizawa (Jichi Medical University)

Magnifying Endoscopy with FICE

Boundary
Vasculature
Magnifying
Vasculature and Magnification
Pathological
Enteroscopy
Transnasal

Stomach

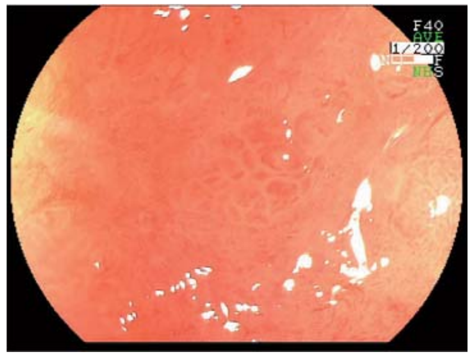

Conventional magnified image

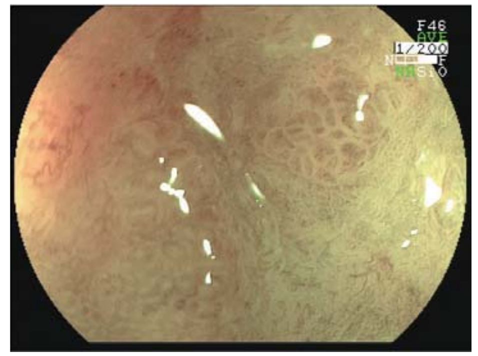

Wavelength

Prototype	R:540	G:415	B:415

Site : Stomach
Case : Early gastric cancer, 0-IIc, well-differentiated adenocarcinoma (tub1 > tub2), 8×8 mm in size, sm (550 um in depth)
Findings : Type IIc + IIa lesion in the greater curvature of the pyloric antrum. Magnifying endoscopy with FICE shows abnormal mucosal pit pattern and tumor vessels.

Photographs provided by Dr. Mitsufuji (Kyoto Prefectural University of Medicine)

Stomach

Conventional magnified image

Wavelength

Prototype	R:555	G:500	B:445

Site : Stomach
Case : Early gastric cancer, 0-IIc, signet-ring cell carcinoma
Findings : Type 0-IIc lesion in the greater curvature of the lower body of the stomach. Compared with conventional magnifying endoscopy, the use of FICE allows clear visualization of the nonstructural pattern in the depressed lesion (disappearance of the fine mucosal pattern) and irregular tumor vessels.

Photographs provided by Dr. Mitsufuji (Kyoto Prefectural University of Medicine)

Stomach

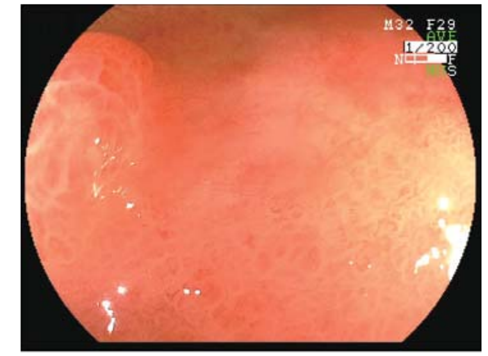

Conventional magnified image

Wavelength

Prototype	R:540	G:500	B:445

Site : Stomach
Case : Early gastric cancer, 0-IIc, well-differentiated adenocarcinoma (tub1 > tub2), 11×7 mm in size
Findings : Type IIc early gastric cancer in the anterior wall of the upper body of the stomach. Compared with conventional magnifying endoscopy, the use of FICE allows clear visualization of the nonstructural mucosal pattern in the depressed lesion (disappearance of the fine mucosal pattern) as well as large and small tumor vessels.

Photographs provided by Dr. Mitsufuji (Kyoto Prefectural University of Medicine)

Large intestine

Conventional magnified image

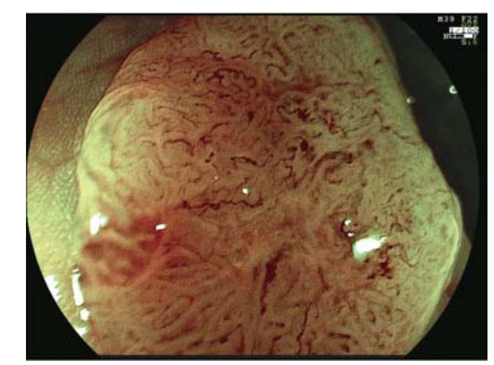

Wavelength

Prototype	R:530	G:455	B:455

Site : Large intestine
Case : IIa + IIc, well differentiated adenocarcinoma
Findings : Magnifying endoscopy with FICE facilitates identification of a irregularity of superficial capillary.

Photographs provided by Dr. Yoshida (Hiroshima University)

Boundary
Vasculature
Magnifying
Vasculature and Magnification
Pathological
Enteroscopy
Transnasal

Magnifying Endoscopy with FICE

Large intestine

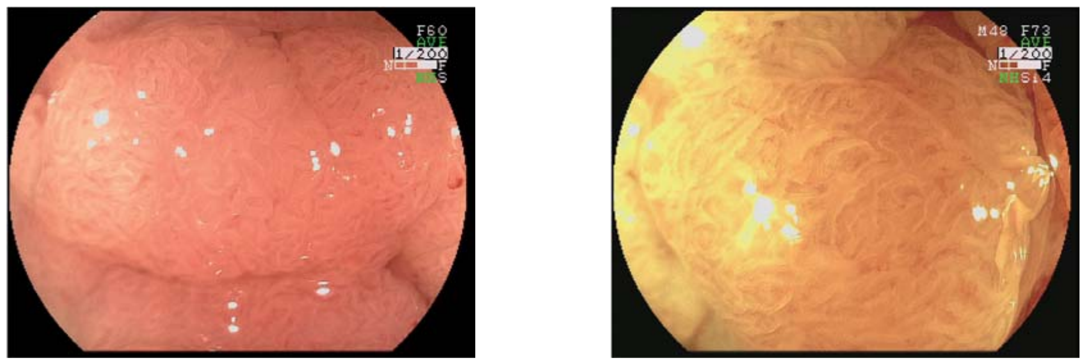

Conventional magnified image

Wavelength

Prototype R:560 G:500 B:475

Site : Large intestine

Case : Laterally spreading tummor (LST), adenoma with moderate atypia

Findings : LST-G (LST, granular type) in the ascending colon. FICE clearly visualizes uniform, meshed pattern vessels, suggesting tubular adenoma. It is found to be adenoma with moderate atypia.

Photographs provided by Dr. Mitsufuji (Kyoto Prefectural University of Medicine)

Large intestine

Conventional image

Wavelength

Prototype R:540 G:490 B:420

Site : Large intestine

Case : Adenoma

Findings : Is, severe atypical tubular adenoma 10 mm in diameter. FICE significantly improves the visibility of the lesion. Magnifying endoscopy clearly shows the boundary between the normal mucosa and adenomatous area.

Photographs provided by Dr. Togashi (Jichi Medical University)

Large intestine

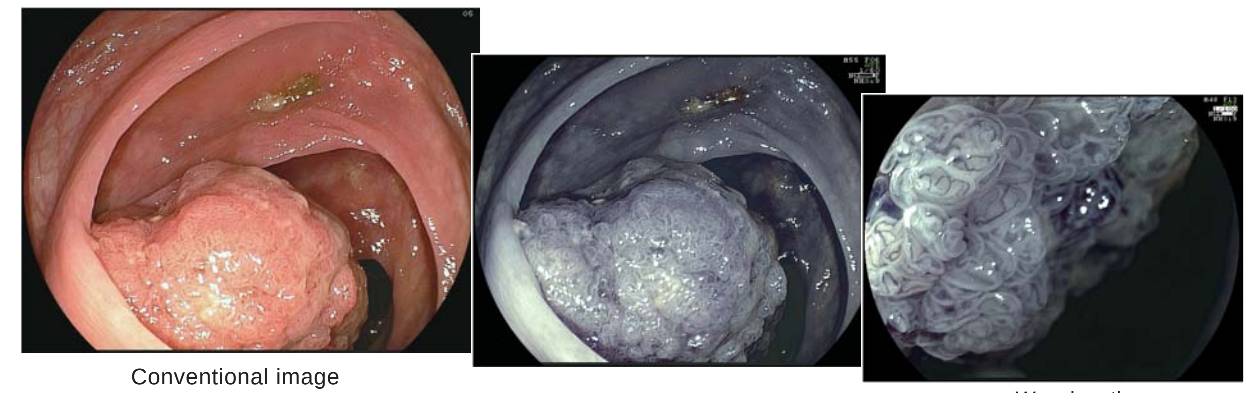

Conventional image

Wavelength

Prototype R:520 G:500 B:405

Site : Large intestine

Case : Isp, moderately differentiated adenocarcinoma in tubulovillous adenoma

Findings : Magnifying endoscopy with FICE clearly visualizes regular microvessels.

Photographs provided by Dr. Yoshida (Hiroshima University)

Large intestine

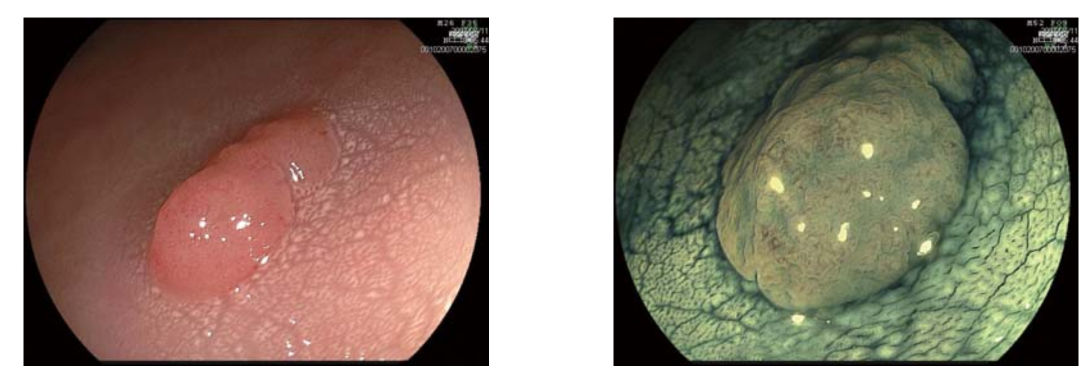

Conventional image

Wavelength (gain)

Pattern: 4 R:520(2) G:500(2) B:405(3)

Site : Large intestine (Ra)

Case : Is, Intramucosal carcinoma (tubular adenoma including intramucosal adenocarcinoma) 12 × 7 mm

Findings : Lobular, elevated lesion. FICE allows clearer visualization of the lesion. The mucosal lesion is most likely carcinoma.

Photographs provided by Dr. Mitooka (Ashiya Mitooka Clinic)

Vasculature and Magnification

Classification of microvascular patterns in esophageal lesions by magnifying endoscopy

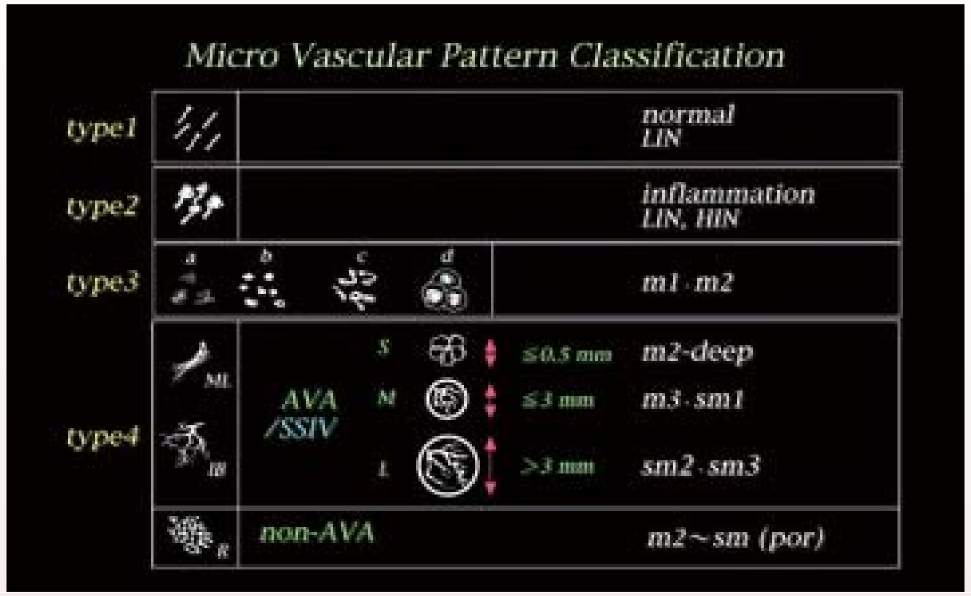

Classification of microvessels in esophageal lesions allows estimation of histopathological features from the appearance of blood vessels, differentiation between benign and malignant diseases, and estimation of the depth of invasion. Microvascular patterns are largely classified into the following four types:

type 1 : Thin, linear capillaries in the subepithelial papilla with less atypical epithelia.

type 2 : Distended, dilated vessels with branched or spiral enlargement. The vascular structure and arrangement are regular. This type is associated with inflammatory changes.

type 3 : Destruction of vessels in the subepithelial papilla, spiral vessels with an irregular caliber, and crushed vessels with red spots. The arrangement of the vessels was irregular. type 3 was generally seen in m1 or m2 cancers.

Subtypes are as follows:

3a : broken filamentous vessels
3b : crushed vessels with red spots
3c : subtype 3b with elongated or fusion
3d : dilated spiral vessels in papillary protrusions with stroma aggregated like salmon roe

type 4 : Characterized by multi-layered (ML), irregularly branched (IB), reticular vessels with an irregular caliber (R),and generally seen in cancers with m2 or deeper invasion.

The size of avascular areas (AVAs) surrounded by type 4 vessels could be used to predict the depth of tumor invasion. In a large AVA, abnormal blood vessels appear, which form a surrounded area with stretched irregular vessels (SSIV). The size of AVA and SSIV may be used to estimate the depth of invasion. There are the following three subtypes.

4S : 0.5 mm or less
4M : 3 mm or less
4L : greater than 3 mm

Vascular patterns are related to the differentiation of carcinomas. Type 4R is often found in poorly differentiated carcinomas.

Provided by Dr. Arima (Saitama Cancer Center)

Normal esophageal mucosa

Conventional image

Wavelength (gain)

Pattern: M R:525(3) G:495(4) B:495(3)

Findings : Network-like vessels under the epithelial layer observed by conventional examination exist mostly in the lamina propria mucosa (lpm). These vessels branch from thicker vessels deep in the submucosal layer.

Photographs provided by Dr. Arima (Saitama Cancer Center)

Magnified image of normal esophageal mucosa

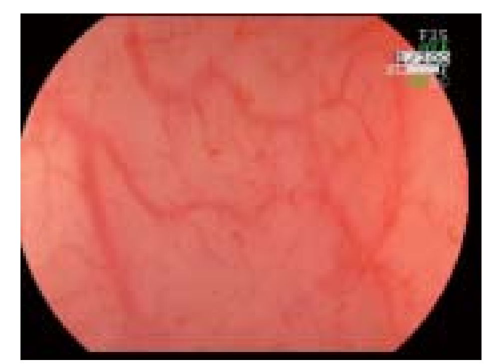

Conventional magnified image

Wavelength (gain)

Pattern: M R:525(3) G:495(4) B:495(3)

Findings : Intra-subepithelial papillary vessels observed in normal esophageal mucosa are thin, loop-like capillaries that originate from network-like vessels in the lpm, rising toward the subepithelial papillae. Intra-subepithelial papillary vessels exist in the subepithelial papillae and are subepithelial vessels in the lamina propria mucosae forming papillae. They are capillaries 10 to 15 μm in diameter that supply blood to the epithelium.

Photographs provided by Dr. Arima (Saitama Cancer Center)

Vasculature and Magnification

Reflux esophagitis (microvascular pattern type 2)

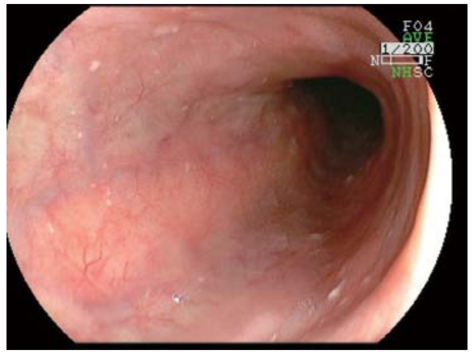

Conventional image

Conventional magnified image

Wavelength (gain)

Pattern: M R:525(3) G:495(4) B:495(3)

Findings : Slightly opaque, mild esophagitis with unclear blood vessels. In magnifying endoscopy, vessels are extended with enlarged and branched ends and increased density. The vascular structure is not destructed, and the arrangement is regular.

Photographs provided by Dr. Arima (Saitama Cancer Center)

Type 0-IIb esophageal cancer Depth of invasion m1 (microvascular pattern type 3a)

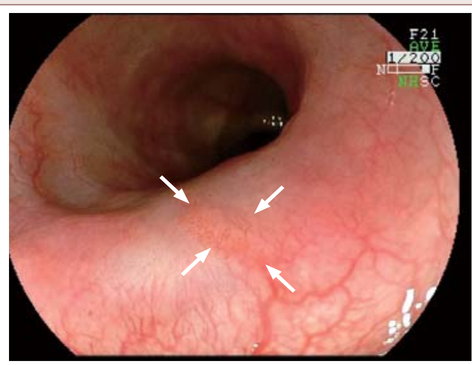

Conventional image

Conventional magnified image

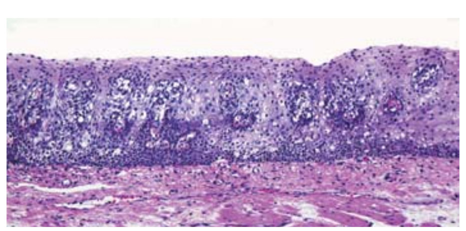

Histopathological image

Wavelength (gain)

Pattern: M R:525(3) G:495(4) B:495(3)

Findings: Erythematous area at the six o'clock position (arrow) leads to recognition of the lesion. In magnifying endoscopy, the broken filamentous microvessels were densely aggregated (type 3a). The vessels are dense, and the structure is irregular. The lesion is basal layer-type carcinoma in situ (m1 carcinoma).

Photographs provided by Dr. Arima (Saitama Cancer Center)

Type 0-IIc esophageal cancer Depth of invasion m1 (microvascular pattern type 3b)

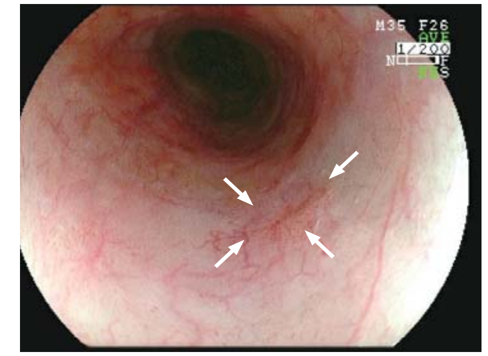

Conventional image

Conventional magnified image

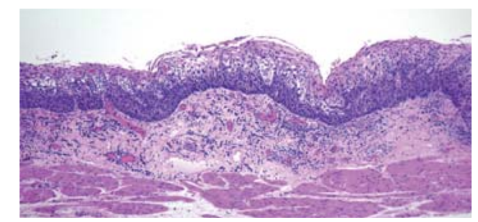

Histopathological image

Wavelength (gain)

Pattern: M R:525(3) G:495(4) B:495(3)

Findings: Slightly erythematous area at the five o'clock position (arrow) leads to recognition of the lesion. The periphery of the erythematous area interrupts the background vessels. In magnifying endoscopy, irregular, crushed vessels with red spots are densely arranged (type 3b), leading to diagnosis of ml carcinoma. EMR revealed the depth of invasion of m1.

Photographs provided by Dr. Arima (Saitama Cancer Center)

Type 0-IIc esophageal cancer Depth of invasion m2 (microvascular pattern type 4S)

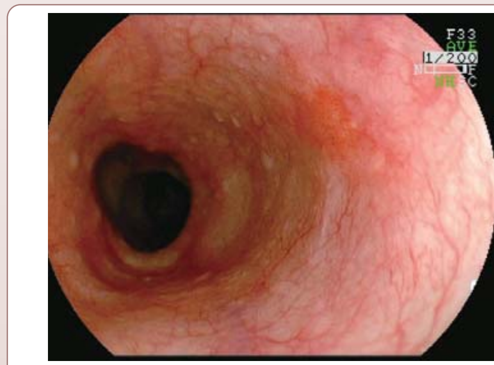

Conventional image

Conventional magnified image

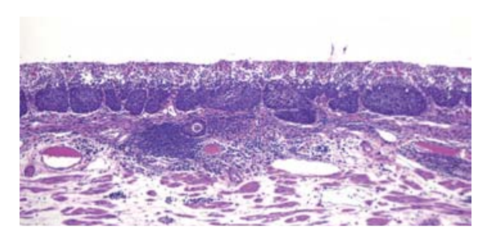

Histopathological image

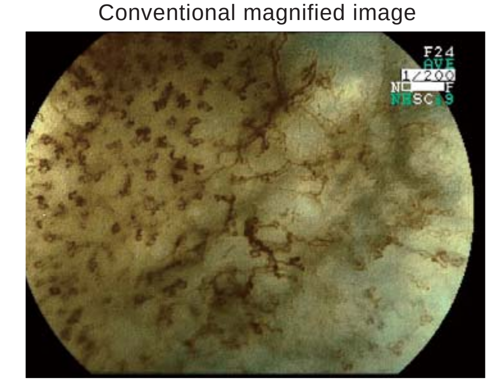

Wavelength (gain)

Pattern: M R:525(3) G:495(4) B:495(3)

Findings: Erythematous area of 10 mm size at the two o'clock position leads to recognition of the lesion. In magnifying endoscopy, irregular, crushed vessels with red spots (type 3b) are densely arranged. Proximally from the center of the lesion, irregularly branched (4IB) and multi-layered (4ML) vessels surround a discolored small AVAs. The AVAs were estimated as 200 - 300 µm. EMR revealed the depth of invasion of m2.

Photographs provided by Dr. Arima (Saitama Cancer Center)

Type 0-IIc esophageal cancer Depth of invasion sm2 (microvascular pattern type 4L)

Conventional image

Wavelength (gain)

Pattern: M R:525(3) G:495(4) B:495(3)

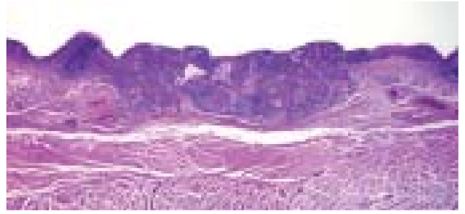

Histopathological image

Findings : 0-IIc lesion associated with elevated margin on the right wall. In magnifying endoscopy, many irregularly branched vessels (4IB) are aggregated in the thickened depressed area, forming an SSIV. The SSIV is greater than 3 mm, which is classified as type 4L. Radical operation revealed the depth of invasion of sm2.

Photographs provided by Dr. Arima (Saitama Cancer Center)

Pathological Diagnosis Using FICE

This chapter presents cases in which a pathological diagnosis is made with the use of FICE.

Pathological Diagnosis Using FICE

Stomach

Conventional image

Wavelength (gain)

Pattern: M R:525(4) G:495(3) B:495(1)

Site : Stomach

Case : Discolored IIc lesion in the gastric corpus

Findings : A IIc lesion in the gastric corpus appears yellow. The depressed yellow lesion is clearly visible on the close, frontal FICE image of the lesion. The histological diagnosis is well-differentiated tubular adenocarcinoma.

Photographs provided by Dr. Kouzu (Chiba University)

Stomach

Conventional image

Wavelength (gain)

Pattern: M R:525(4) G:495(3) B:495(1)

Site : Stomach

Case : Lesion with both elevated and depressed areas in the greater curvature of the gastric corpus

Findings : IIa + IIc lesion in the gastric corpus.

The FICE image clearly shows a yellowish change in the boundary. After a biopsy, the diagnosis is a well-differentiated tubular adenocarcinoma. In this case, the boundary of the lesion is clearly visible.

Photographs provided by Dr. Kouzu (Chiba University)

Stomach

Conventional image

Wavelength (gain)

Pattern: M R:525(4) G:495(3) B:495(1)

Site : Stomach

Case : Elevated lesion in the cardia of the stomach

Findings : IIa lesion. The FICE image clearly shows the boundary and surface irregularity.

Photographs provided by Dr. Kouzu (Chiba University)

Pathological Diagnosis Using FICE

Stomach

Conventional image

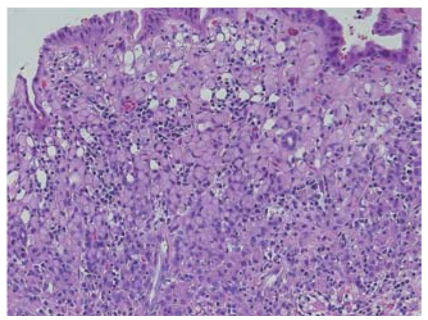

Histopathological image

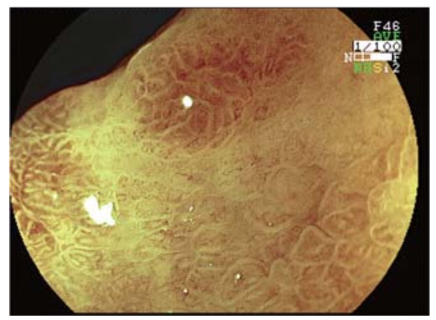

Wavelength (gain)

Pattern: M R:550(2) G:500(5) B:470(4)

Site : Stomach
Case : Early gastric cancer, 0-IIc, signet ring cell carcinoma.
Findings : The reddish mucosa associated with the deformation of greater curvature of the gastric angle. On the conventional endoscopic image, a slightly reddish mucosal change in the greater curvature of the gastric angle is observed. The reddish change is enhanced on the FICE image. Magnifying endoscopy with FICE shows irregular microvascular pattern and irregular microstructural pattern. The histological diagnosis is signet ring cell carcinoma.

Photographs provided by Dr. Osawa and Dr. Yoshizawa (Jichi Medical University)

Large intestine

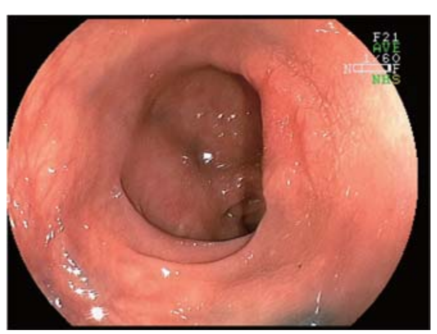

Conventional image

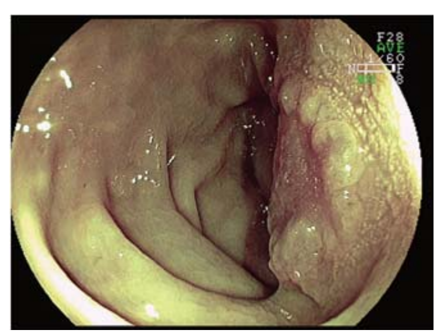

Wavelength

Prototype R:540 G:490 B:420

Site : Large intestine
Case : Elevated lesion covering one-third of the lumen.
Findings : Non-granular type laterally spreading tumor (LST-NG) 19 × 15 mm in diameter, well-differentiated adenocarcinoma (depth of invasion is m).
LST-NG, which is not clear on the conventional image, is clearly shown with the use of FICE.

Photographs provided by Dr. Togashi (Jichi Medical University)

FICE booth lecture

Dr. Herbert Burgos (Gastroclinica, Costa Rica) lecturing on FICE at Fujinon's booth during DDW 2007, USA

Enteroscopy with FICE

This chapter presents cases in which enteroscopy with FICE was useful for diagnosis.

Small intestine

Conventional image

Wavelength

Prototype	R:555	G:500	B:445

Site : Small intestine

Case : Observation of villus in the small intestine

Findings : A case of blind loop syndrome that developed due to hypoproteinemia and iron deficiency anemia about 30 years after bypass surgery with side-to-side anastomosis of the ileum for treatment of adhesive intestinal obstruction. Compared with the conventional image, the erythematous change of the small intestinal villi on the ulcer edge is more clearly visible in the FICE image.

Photographs provided by Dr. Yano (Jichi Medical University)

Small intestine

The ulcer base observed during the previous examination

Conventional image

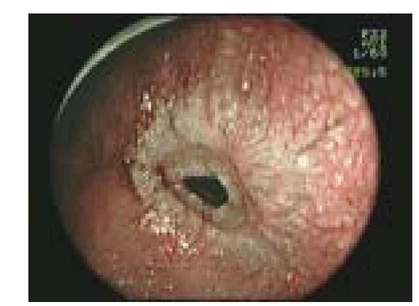

Wavelength

Prototype	R:555	G:500	B:445

Site : Small intestine

Case : Small intestine ulcer

Findings : A case of non-Hodgkin B-cell lymphoma that was treated by seven courses of R-CHOP chemotherapy eight months ago. The ulcer base observed during the previous examination disappeared. The whitish scar is more clearly visible compared with the surrounding area with the use of FICE.

Photographs provided by Dr. Yano (Jichi Medical University)

Transnasal Endoscopy with FICE

This chapter presents cases in which transnasal endoscopy with FICE is useful for diagnosis.

Transnasal Endoscopy with FICE

Stomach

Conventional image

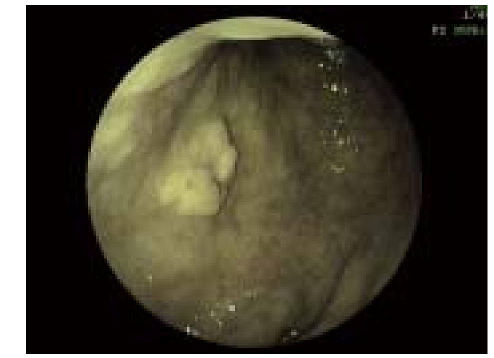

Wavelength (gain)

Pattern: M R:525(4) G:495(5) B:495(4)

Site : Anterior wall of the body of the stomach

Case : Gastric adenoma

Findings : White granular elevations approximately 10 mm in diameter are found in the anterior wall of the body of the stomach. Compared with the conventional image, contrast of the lesion is more enhanced, and the boundary of the adenomatous area is more clearly visible on the FICE image.

Photographs provided by Dr. Yanai and Dr. Tanioka (Kanmon Medical Center)

Stomach

Conventional image

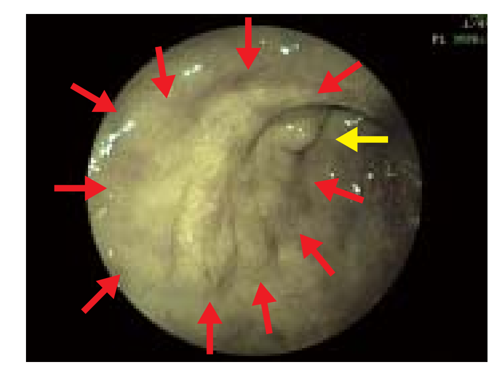

Wavelength (gain)

Pattern: M R:525(4) G:495(5) B:495(4)

Site : Gastric antrium

Case : Early gastric cancer

Findings : On the conventional image, a partially elevated tumor is observed near the pyloric ring. The FICE image reveals milder elevations extending to the surrounding area.

Photographs provided by Dr. Yanai and Dr. Tanioka (Kanmon Medical Center)

Transnasal Endoscopy with FICE

Boundary
Vasculature
Magnifying
Vasculature and Magnification
Pathological
Enteroscopy
Transnasal

Stomach

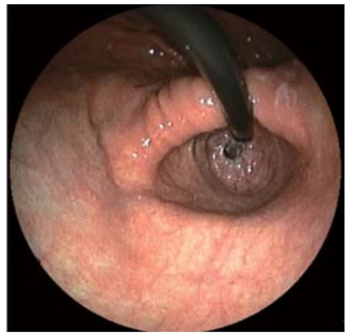

Conventional image

Wavelength (gain)

Pattern: M R:525(3) G:495(4) B:495(3)

Site : Stomach

Case : Gastritis

Findings : Blood vessels in the atrophic gastritis are more clearly visible in the FICE image. This may be useful for recognition of the area of atrophic change of the gastric body mucosa.

Photographs provided by Dr. Yanai and Dr. Tanioka (Kanmon Medical Center)

Stomach

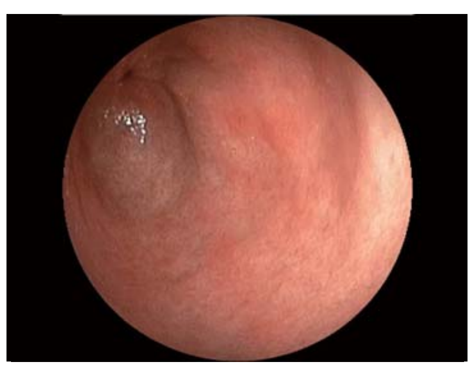

Conventional image

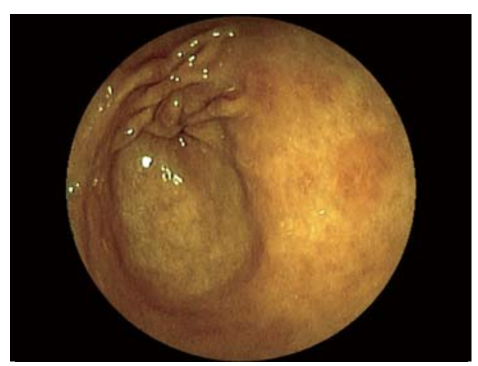

Wavelength (gain)

Pattern: M R:550(4) G:500(5) B:470(3)

Site : Stomach

Case : Gastritis

Findings : Verrucous erosion in the erosive gastritis is clearly visible.

Photographs provided by Dr. Yanai and Dr. Tanioka (Kanmon Medical Center)

Stomach

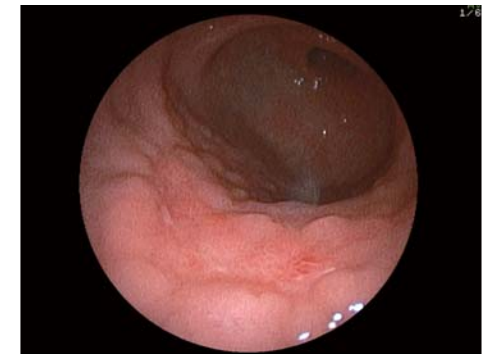

Conventional image

Wavelength (gain)

Pattern: 2 R:550(2) G:500(2) B:470(3)

Site : Stomach

Case : gastric cancer

Findings : The FICE image clearly shows the surface irregularity of the depressed area and fold convergence in the surrounding area in type IIc gastric cancer.

Photographs provided by Dr. Miyawaki (Izumo Central Clinic)

Stomach

Conventional image

Wavelength (gain)

Pattern: 2 R:550(2) G:500(2) B:470(3)

Site : Stomach

Case : gastric cancer

Findings : The FICE image enhances the surface pattern of gastric cancer with a depressed lesion IIc in the greater curvature of the gastric corpus.

Photographs provided by Dr. Miyawaki (Izumo Central Clinic)

Boundary
Vasculature
Magnifying
Vasculature and Magnification
Pathological
Enteroscopy
Transnasal

Transnasal Endoscopy with FICE

Stomach

Conventional image

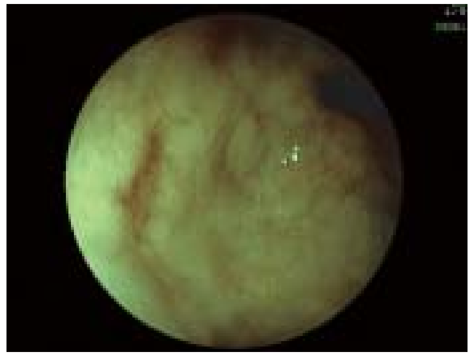

Wavelength (gain)

Pattern: M R:550(2) G:500(5) B:470(4)

Site : Gastric antrum

Case : Gastritis

Findings : On the conventional endoscopic image, a mild erythematous change is found in the anterior wall of the antrum. The FICE image enhances its change compared with the conventional image.

Photographs provided by Dr. Osawa (Jichi Medical University)

Duodenum

Conventional image

Wavelength (gain)

Pattern: M R:550(2) G:500(5) B:470(4)

Site : Duodenum

Case : Erosion

Findings : Erosions are found in the anterior wall of the duodenal bulb. Compared with the conventional image, the reddish mucosal changes are enhanced on the FICE image.

Photographs provided by Dr. Osawa (Jichi Medical University)

Notes